Behavior of Steel Reduced Beam Web (RBW) Connections with Multi Longitudinal Voids

Sepanta Naimi

Submitted to the
Institute of Graduate Studies and Research
in Partial fulfillment of the requirements for the degree of

Doctor of Philosophy
in
Civil Engineering

Eastern Mediterranean University
October 2013
Gazimağusa, North Cyprus

Approval of the Institute of Graduate Studies and Research

Prof. Dr. Elvan Yılmaz
Director

I certify that this thesis satisfies the requirements as a thesis for the degree of Doctor of Philosophy in Civil Engineering.

Prof. Dr. Özgür Eren
Chair, Department of Civil Engineering

We verify that we have read this thesis and that in our opinion it is fully adequate in scope and quality as a thesis for the degree of Doctor of Philosophy in Civil Engineering.

Asst. Prof. Dr. Amir Ahmad Hedayat
Co-Supervisor

Asst. Prof. Dr. Mürüde Çelikağ
Supervisor

Examining Committee

1. Prof. Dr. Ayşe Daloğlu
2. Assoc. Prof. Dr. Zalihe Sezai
3. Asst. Prof. Dr. Erdinç Soyer
4. Asst. Prof. Dr. Giray Özay
5. Asst. Pror. Dr. Mürüde Çelikağ

ABSTRACT

Since the earthquakes in Northridge and Kobe in 1994 and 1995 respectively, many investigations have been carried out towards improving the strength and ductility of steel beam to column pre and post-Northridge connections. In order to achieve these objectives recent researches are mainly focused on three principles; reducing the beam section to improve the beam ductility, adding different kinds of slit damper to beam and column flanges to absorb and dissipate the input earthquake energy in the connection and strengthening the connection area using additional elements such as rib plates, cover plates and flange plates to keep the plastic hinges away from the column face. This research presents a reduced beam section approach via the introduction of multi longitudinal voids (MLV) in the beam web for various beam depths varying from 450mm to 912mm. ANSYS finite element program was used to simulate the three different sizes of SAC (Structural Engineering Association of California) sections, SAC3, SAC5 and SAC7. Then the modification was applied to these post-Northridge SAC sections. Results showed an improvement in the connection ductility since the input energy was dissipated uniformly along the beam length and the total rotation of the connection was over four percent radian.

Keywords: Multi-Longitudinal Voids; Strength; Ductility; post-Northridge connection.

ÖZ

Northridge ve Kobe'de sırasıyla 1994 ve 1995 yıllarında meydana gelen depremler sonrasında Northridge öncesi ve sonrası, çelik kolon-kiriş bağlantılarının dayanım ve sünekliğini artırmak için birçok araştırma yapılmıştır. Bu amaçlara ulaşmak için son zamanlarda araştırmacılar üç ana prensibe odaklı çalışmaktadırlar; kirişin sünekliğini kiriş gövde kesitini azaltarak iyileştirme, bağlantıda deprem enerjisi girdisini emmek ve dağıtmak için kiriş ve kolon flanjlarına yarık amartisör ekleme, bağlantı bölgesini ek elemanlarla (örneğin, kaburga plakası, plaka kapağı ve flanj plakası kullanarak) güçlendirme ve bu yaklaşımla plastik mafsalı kolon yüzünden uzak tutma. Bu araştırmada, sunulan kirişin sünekliğini kiriş gövde kesitini azaltarak iyileştirme prensibini kullanarak, kiriş yükseklikleri 450 mm ile 912 mm arasında değişen kiriş gövdelerinde çoklu yatay boşluklar oluşturmadır. ANSYS sonlu elemanlar programı kullanılarak üç farklı boyut SAC kesitini SAC3, SAC5 ve SAC7 modellenmiştir. Bunu takiben yukarıda belirtilen değişiklikler Northridege sonrası SAC kesitlerine uygulanmıştır. Araştırma ve incelemeler, deprem enerji girdisinin kiriş boyunda eşit şekilde dağılması sonucu kolon-kiriş bağlantılarının sünekliğinde iyileşme göstermiştir ve toplam bağlantı rotasyonu yüzde dört radyanı aşmıştır.

Anahtar kelimeler: Çoklu yatay böşluklar, Dayanım, Süneklik, Northridge sonrası bağlantı

To my wife and my parents

ACKNOWLADGMENT

I would like to thank Asst. Prof. Dr. Mürüde Çelikağ for her valuable contributions in terms of supervision, advice and encouragement right from the conception of this dissertation to the very end. Her time, ideas, and experiences have really strengthened and motivated me to work harder. I must confess that she has been like my mother. Therefore, I thank her from the bottom of my heart.

My special thanks go to my Co- Supervisor Asst. Prof. Dr. Amir Ahmad Hedayet for his valuable support from the beginning of this dissertation to the end. He is my very good friend who has shown what true friends are through his advice, encouragement, knowledge and experience. Big hearth-full thanks to him.

I would also like to thank Asst. Prof. Dr. Erdinç Soyer and Asst. Prof. Dr. Giray Özay for their contributions to this study. Being part of my thesis follow up committee, their advice and criticism helped a lot for the improvement of this research.

I am also grateful to Asst. Prof. Dr. Mustafa Ergil, Assoc. Prof. Dr. Umut Türker and Assoc. Prof. Dr. Zalihe Sezai for creating conducive working environment that enabled me to develop myself in class lecturing towards becoming a better instructor.

It is from my heart to thank Saeid Moazam, Olusegun A. Olugbade and Aidin Shojaeirad for their support for this thesis.

My gratitude is extended to my wonderful parents for their unconditional love, support and encouragement which really motivated me to complete this study. I adore you both.

Finally, special appreciation goes to my wife for her love, care, patience and support throughout this study. I love you with all my heart and I really thank you.

TABLE OF CONTENTS

LIST OF TABLES

LIST OF FIGURES

LIST OF ABBRIVATIONS

RBW	Reduced Beam Web
MLV	Multi Longitudinal Voids
WAH	Weld Access Hole
BEC	Beam End Configuration
CJP	Complete Joint Penetration
PEEQ	Plastic Equivalent Strain
WSMF	Welded Steel Moment Frame
SMRF	Steel Moment Resisting Frame
SFRS	Seismic Force Resisting System
RBS	Reduced Beam Section
RBW	Reduced Beam Web
MLV	Multi Longitudinal Voids

Chapter 1

INTRODUCTION

1.1 Introduction

Observations after the earthquakes in Northridge (1994) and Kobe (1995) (Mahin, 1998) revealed that welded connections of Steel Moment Resisting Frames (SMRF) suffered brittle fractures. Northridge Earthquake has shown variety of fractures at welded moment connections. The most common fractures were initiated at the Complete Joint Penetration (CJP) weld root of the beam flange and expanded to the column web and flange. Figure 1 shows the typical fracture paths of Northridge connections (Popov et al.,1994).

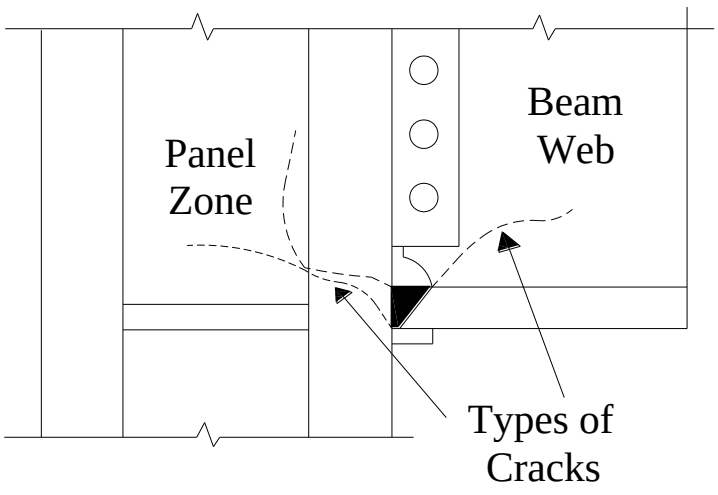

Figure 1: Typical fracture paths at the welded beam-to-column connection (Popov et al., 1998)

Generally, the deep rolled beam and column sections with A36 and A572 steel material respectively are used in Pre-Northridge SMRF design. In order to transfer

shear forces a bolted shear tab is used, and to join the beam flange to the column flange a CJP groove weld is used in the field. The weld metal (for example, 483 MPa (70 ksi)) was chosen to overmatch the base metal, nominal A36 steel beam. Any weld metal toughness, welding process and practice could have been used. Under SAC program twelve specimens were selected for laboratory test verification (W30×99 and W36×150). The test results showed that the Pre-Northridge moment connections had a very low performance under cyclic loading because of inadequate ductility (Phase 1) (SAC 1996).

In 1994, the new code is accepted as the seismic design standard by California jurisdictions. Before 1994, the Uniform Building Code (UBC) was presumed that for Pre-Northridge connections only strength can satisfy the beam-to-column connection requirements (ICBO 1994). Ductility of Pre-Northridge connections have been investigated through several tests by a number of researchers between 1969 and 1984 (Popov et al. 1969, Popov et al. 1970, Popov et al. 1972, Popov et al. 1973, Carpenter et al. 1973, Beedle et al. 1973, Chen el al. 1981). The results showed that only the shallow specimens (W18×50 and W24×76) were adequate to achieve minimum 0.04 rad total rotation.

Since then modifications to design procedure of Pre-Northridge connections and its welding type has been introduced. E70T-4 type welding was changed to E70-TGK2 with smooth welding access holes and the backing bar was removed from the bottom beam flange (Miler, 1998 and Lee et al., 2001). This type of connection is now known as post-Northridge connection. The typical pre-Northridge connection is shown in Figure 2 and the typical post-Northridge connection that is used in this research are shown in Figure 3 (a, b and c)

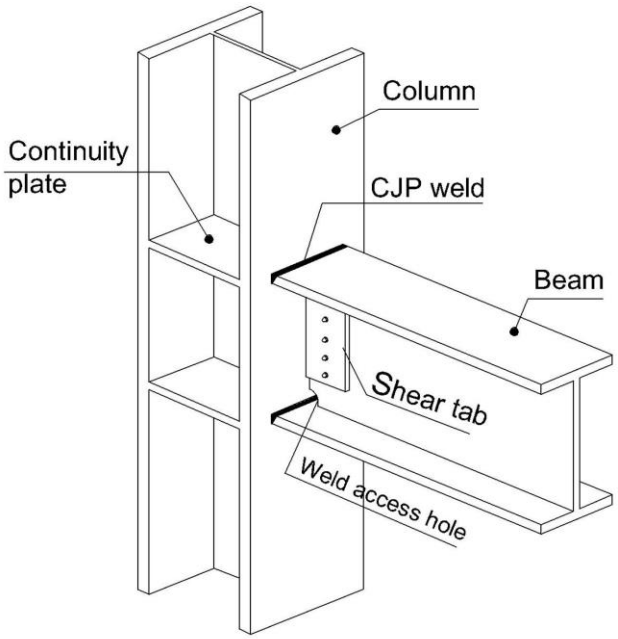

Figure 2: Typical connection for pre-Northridge SMRF

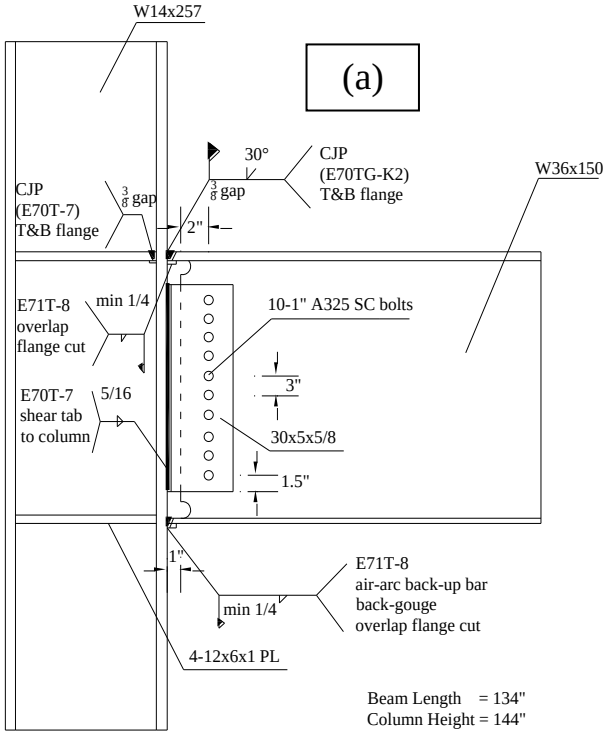

(a)

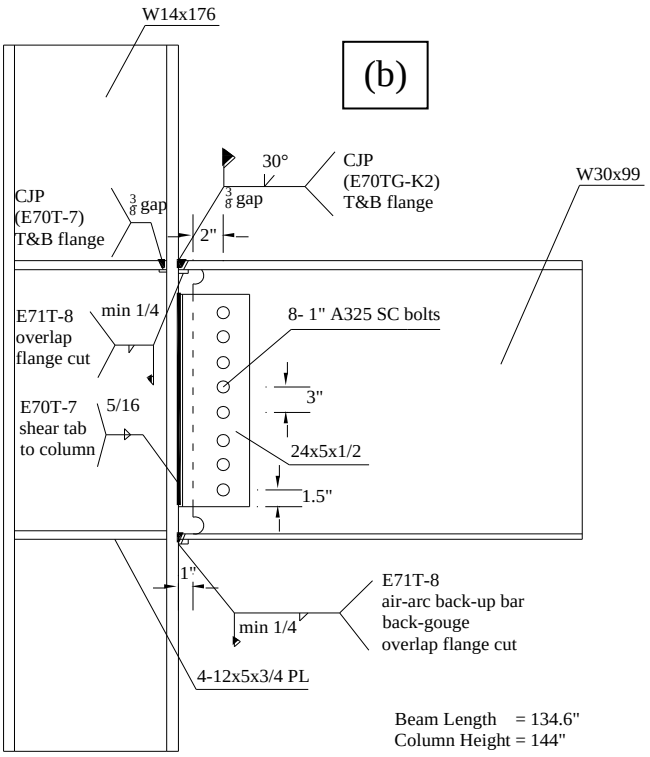

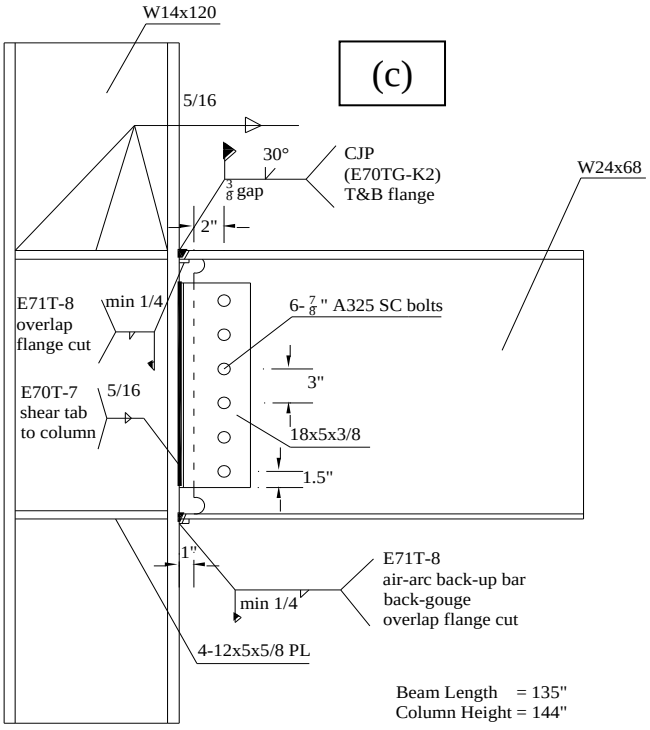

Figure 3: SAC specimens utilized by Lee (2000): (a) SAC7; (b) SAC5; (c) SAC3

Three principles are mainly used to improve the strength and ductility of the post-Northridge connections:

1. Strengthening of connection by adding additional elements including cover plates and flange plates (Engelhardt and Sabol, 1998),(Kim et al.,2000), triangular haunches (Chia et al., 2006), straight haunches (SAC, 1996), upstanding ribs (Popov and Tsai, 1998), lengthened ribs (Chen et al., 2003), side plates (Engelhardt and Sabol, 1994) and bolted brackets (Chen et al., 2004) and (Kasai and Mao, 1997).

2. Reducing the beam section to improve the beam ductility so that the stress concentration will transfer to a region away from the connection. Reduction of beam section can be done by reducing the flange section (Reduce Beam Section, RBS (Popov et al., 1998) or by reducing the web section (Reduce Beam Web, RBW). Among the RBW connections are the introduction of wedge design at the beam bottom flange and web (Wilkinson et al., 2006) and (Hedayat and Celikag, 2010) and reducing the beam web are by opening circular voids (Ascheheim, 2000) and (Hedayat and Celikag, 2010), rectangular long voids (Hedayat and Celikag, 2009), drilled voids (Hedayat and Celikag, 2011), and RBW with arch-shape cuts at the beam web (Hedayat and Celikag, in press).

3. Adding different kinds of slit damper plates to beam and column flanges that will absorb and dissipate energy at connections during earthquake (Saffari et al., 2013).

These methods are applied to shift the plastic hinge from the connection area at the face of the column to the beam so that the stress concentration will reduce at the CJP. These modifications must be as such to be applicable for both existing and new buildings. Weakening of the beam section (RBS) at the flange area in existing buildings is difficult and expected to be more costly than reducing the beam web (RBW). This is due to difficulties in accessing the beam top flange and modifying it in the presence of concrete floor.

In 2009, Hedayat and Celikag proposed the use of rectangular long voids at the beam web to improve the plastic rotation capacity of post-Northridge connections (Figure 4). This method was effective for beams with maximum depth equal to 600 mm. However, for deeper beams due to the high level of strain concentration at the RBW area and excessive lateral-torsional buckling of the beam web (which was due to the increase in the depth of the voids) the efficiency of this method reduced and the modified connection did not achieve adequate connection's strength and ductility. Hence, for deep beams, Hedayat and Celikag (2009) proposed adding tube and stiffener at the RBW area. However, the main drawback of this approach is the increase in cost and time consumption to modify the beam.

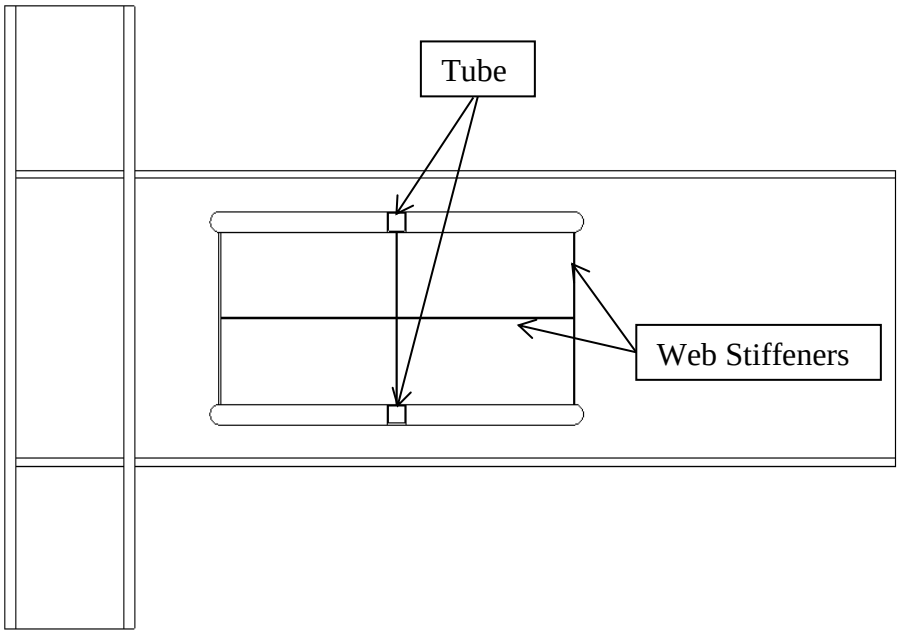

Figure 4: Single longitudinal voids with stiffeners and tube at the center of voids proposed by Hedayat and Celikag (2009)

1.2 Objective of Study

The study covered in this research work was aimed to improve the seismic performance of post-Northridge connections, particularly with deep beams, by creating multi-longitudinal voids at the beam web (Figure 5). When compared to the method presented in reference (Hedayat and Celikag, 2009), the multi longitudinal voids configuration used to reduce the beam web in this research is more economical with less cost and workmanship. This method also can lead to the achievement of a more uniformly distributed strain at the RBW area when compared to the one proposed in reference (Hedayat and Celikag, 2009). To figure out the most suitable connection configuration, a parametric study was done with respect to the size and the location of the voids. 173 models were created using Finite Element Method (FEM) to do the parametric study. The results showed that the connections achieved the minimum 4 percent total rotation and more so in some cases of deep beam sections the connection rotation even exceeded 5 percent total rotation.

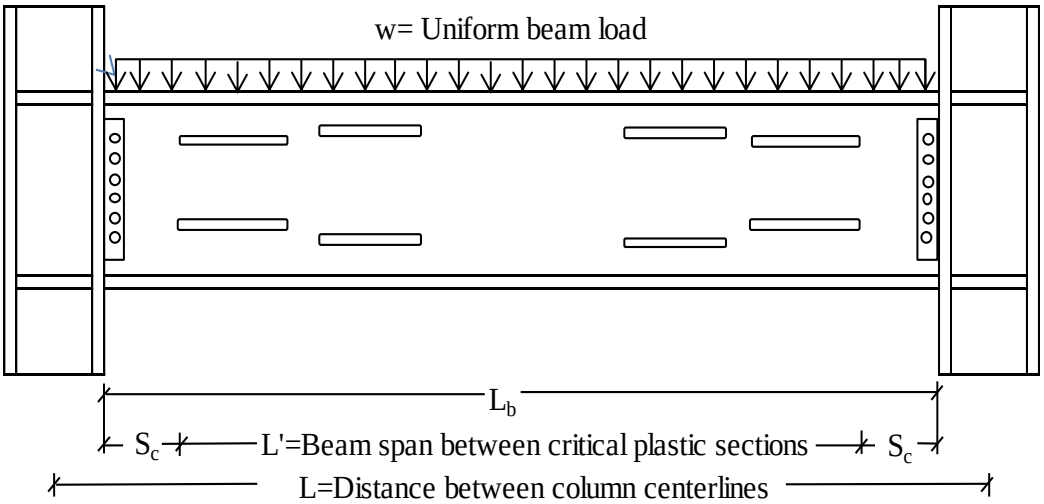

Figure 5: Modified post-Northridge connections with multi longitudinal voids

1.3 Outline of Thesis

This thesis contains six chapters' the details of which are given below:

- **Chapter 2: Literature Review.** Previous analytical and experimental research in this field were investigated together with the SAC group report, AISC 2010 and FEMA350 standards to gather all the past work to highlight the important findings and the need for this particular study.
- **Chapter 3: Methodology.** This chapter presents the possible methods of improving the performance of welded steel moment frames. FEM was used to model a previously tested post-Northridge connection to verify the three different SAC specimens via 29 analytical models. After verification of the SAC model the single pair of voids configuration of Hedayat and Celikag (2009) was also analytically verified. Then the 144 multi longitudinal voids configurations suggested in this study were modeled using the dimensionless parameters introduced in this study.

- **Chapter 4: Analytical results and Discussion.**

  The results of the analysis of the models in Chapter 3 were compared and discussed in this chapter. The results of monotonic and cyclic loading of the modified analytical models were presented and they indicated considerable improvement in the plastic rotation capacity of the connection, with some models exceeding the 5 percent total rotation.

- **Chapter 5: Generalized Design Procedure.**

  This section considers the use of parameters, such as, gravity effect, length of the beam and moment gradient of the beam were neglected, to generalize the design procedure so that the proposed modifications can be applicable to other sections.

- **Chapter 6: Conclusions and Recommendations for Future Work**

  Conclusions drawn from this particular research and recommendations for possible future work to further develop the ductility and the strength of moment connections are given in this chapter.

Chapter 2

LITERATURE REVIEW

2.1 Introduction

After the Northridge earthquake at 1994 the pre and post Northridge connections became one of the most important and popular research areas in steel structures, particularly in countries with seismic activities. These research results lead to new design procedures to be established in design codes to avoid brittle fractures at beam to column connections of steel moment resisting frames (SMRF) (Gates et al., 1994), (Naeim et al., 1994), (Green et al., 1994) and (Hajjar et al., 1995). Post Northridge connections were introduced as a result where the weld material and the shape of the weld access hole were changed, as shown in Figures 6 and 7.

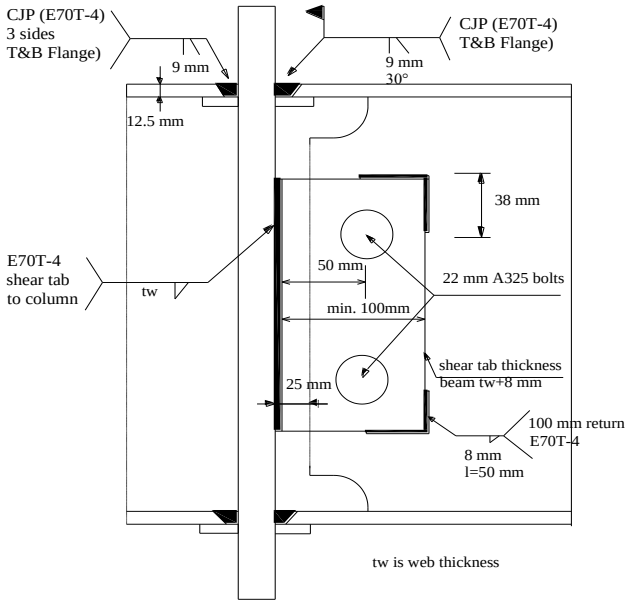

Figure 6: SAC pre-Northridge connection (Lee et al., 2000)

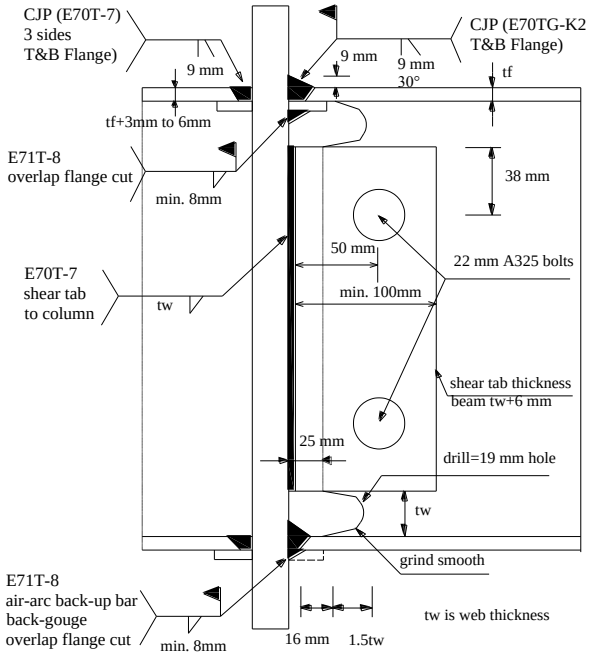

Figure 7: SAC post-Northridge connection (Lee et al., 2000)

Then, many analytical and/or experimental investigations were carried out by researchers to improve on the ductility of post-Northridge connections by either strengthening the column and connection or weakening the beam section. The ultimate aim was to achieve minimum 80 percent of the plastic moment and also minimum 4 percent of the total rotation (Popov (1996), Chen et al. (2005), SAC (1996), Ricles (2002), Lee (2000) and etc.).

Moreover, a number of time hysteresis were used by FEMA (2000) and Chen et al. (2005) to see the behavior of the deep, moderate and shallow beam sections when subject to severe earthquakes (Figures 8 and 9). Figure 10 gives the verification of their analytical results by experimental tests.

It was important to observe from these tests that the analytical monotonic loading results can be verified by cyclic loading results (Chen et al. 2005).

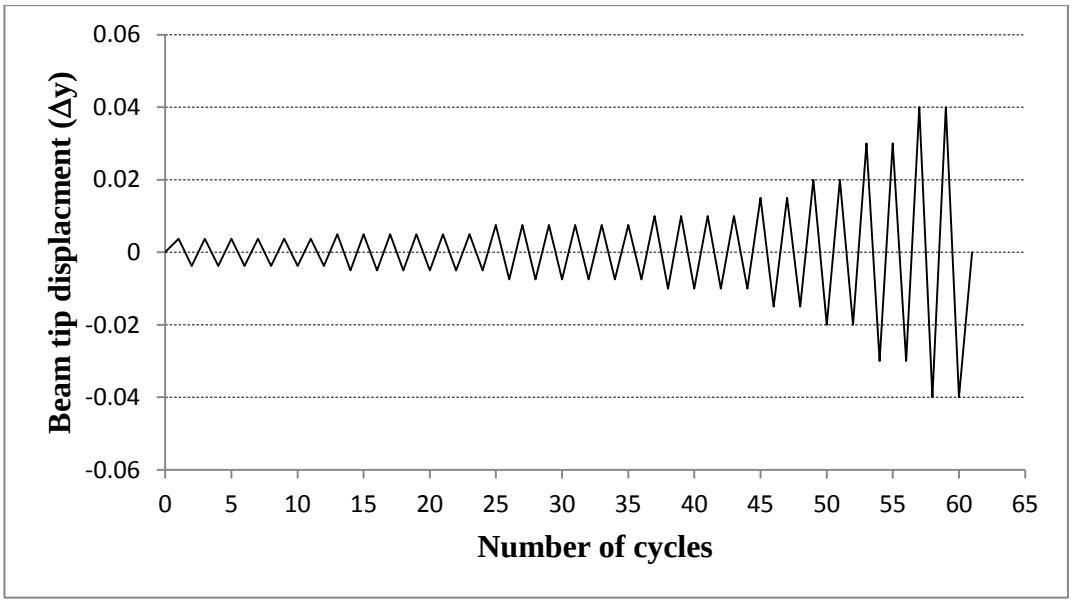

Figure 8: The load history used by FEMA. (2000)

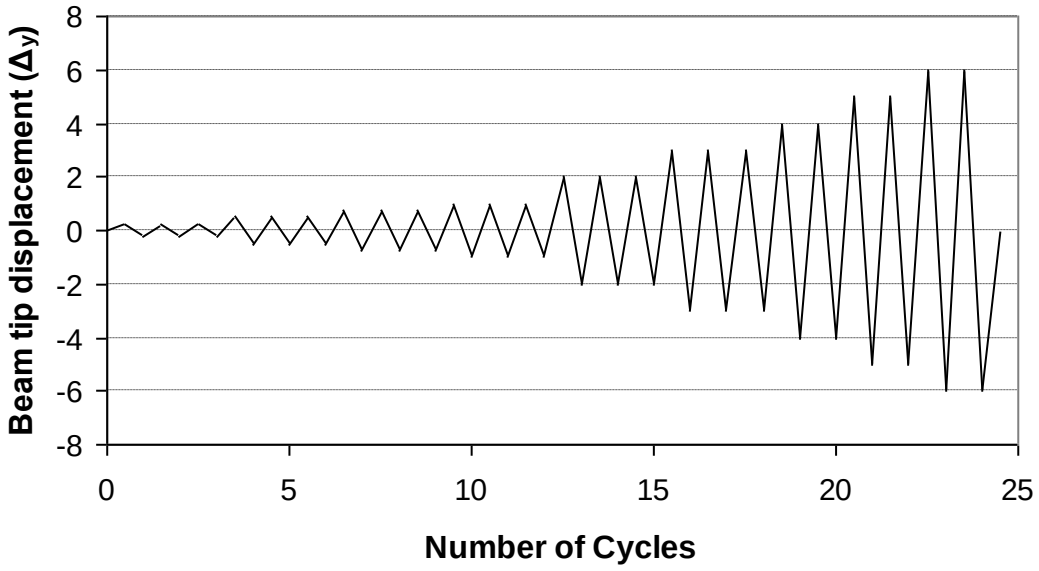

Figure 9: The load history used by Chen et al. (2005)

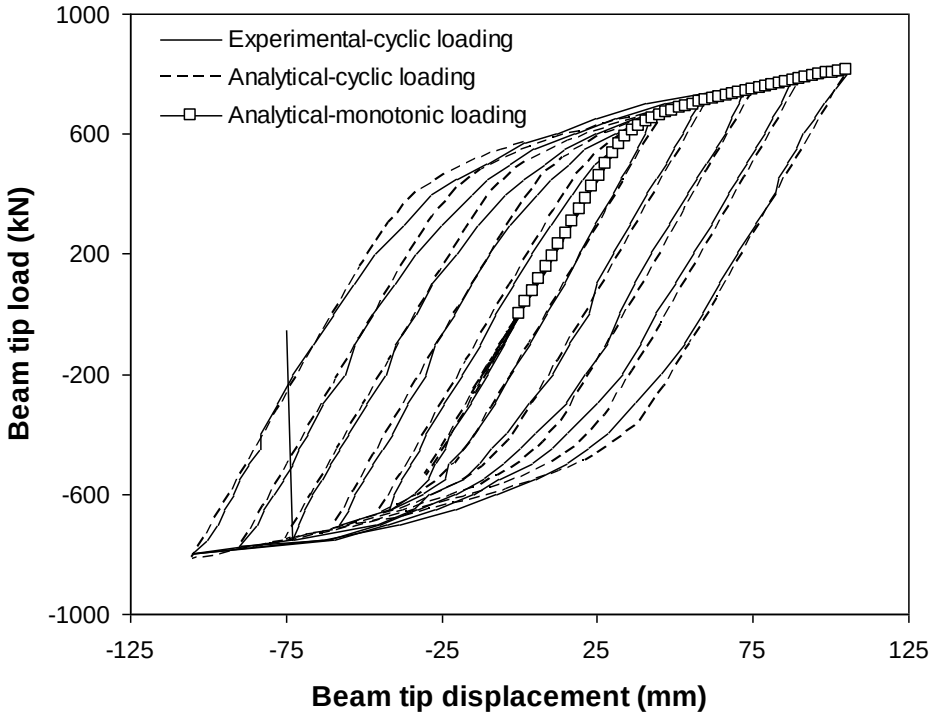

Figure 10: Comparison of experimental (Chen et al. 2005) and analytical hysteresis curves of specimen when subject to cyclic and monotonic loading

2.2 Modification Types

2.2.1 Strengthening the Connection Configuration

The aim of strengthening the post-Northridge moment connection is to improve its performance against severe earthquakes. This method is based on reinforcing the connection so that the connection becomes stronger than the beam and in this way the location of the plastic hinge moves away from the column face. Therefore, this would help to avoid

- Stress concentrations at weld access holes,
- Possible premature fractures resulting from potential weld defects at the connection,
- Stress concentrations caused by column flange bending,
- Triaxial tension due to restraint levels being too high

- Variations in the through-thickness properties of column flange, etc.

Some of the connection reinforcement methods are listed below:

- Cover plates
- Side plates
- Bolted brackets
- Upstanding ribs
- Lengthened ribs
- Triangular haunches
- Straight haunches
- Slit damper

2.2.1.1 Adding Cover Plate

Since 1994 cover plates are the most usual method for strengthening the post-Northridge connection as it is shown in Figure 11.

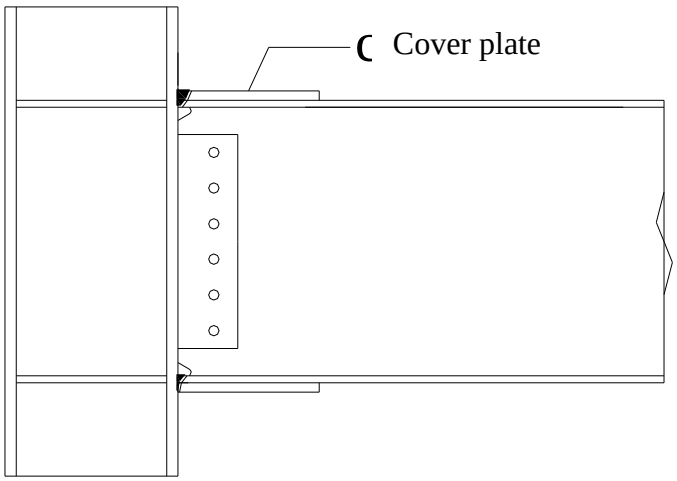

Figure 11: Strengthening of the connection using top and bottom cover plates

The rectangular cover plate that is wider than beam flange is used for the bottom beam flange and the tapered one that is thinner than beam flange is used for the top flange.

A variety of tests were carried out by investigators to find the behavior of reinforced connections by cover plate under cyclic loading (Engelhardt. et al., 1989) and (Tsai et al., 1993). The results showed that using cover plate for shallow beams may cause very high connection cyclic ductility but deep sections may not have this high performance due to premature brittle failure at low plastic rotation (Engelhardt et al., 1998).

2.2.1.2 Adding Side Plates

This type of strengthening is completely different than the other methods, the connection is covered with plates from each sides (top and bottom can also be covered if it is dimensionally needed) to form a physical gap between the column face and the end of the beam (Figure 12). This physical gap will cause the moment transfer from the beam to the column through the Side Plate.

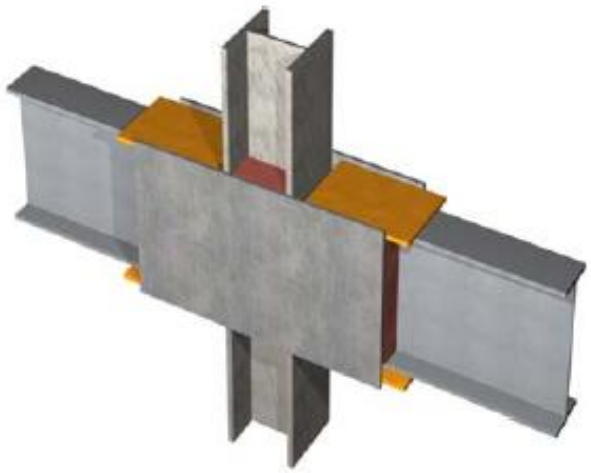

Figure 12: Side Plate Moment connection (Uang 1995)

In 1995 and 1996 Uang (University of California, San Diego) conducted several tests under cyclic loading to verify connection strength; the results have shown that an average of 0.036 radian plastic rotation can be achieve by adding side plate.

In addition, independent investigation by Frank in 1997 had shown that the connections strengthen with side plate are acceptable to be used for buildings, such as, hospitals and courthouses.

On the other hand, the side plate modification may be developed to mitigate the blast effect on the connection to control the collapse of the structure after a possible bomb blast in case of a terrorist attack (Houghton and Karns, 2001 & Crawford et al., 2002).

2.2.1.3 Adding Welded Haunches

Adding welded haunches is another way of strengthening post-Northridge moment connections. There are two types of haunches, Triangle Haunches and Straight Haunches, as shown in Figure 13.

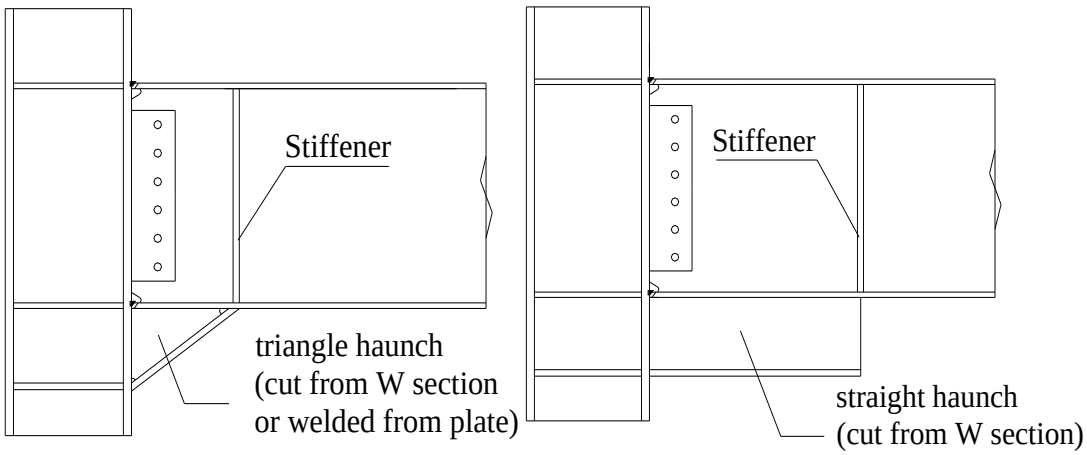

Figure 13: Welded haunches: (a) Triangular; (b) Straight

In this method welded haunch protects the connection weld by increasing the beam section modulus at the column face. Triangular haunches were analytically tested by Yu in 2000. The analytical results obtained from FEM modeling were compared with the experimental test results. The outcome indicated that the haunch transferred more shear of the beam to the column than the groove welds at the column face and bolts at the web connection and helped the beam moment dissipation to the haunch section.

Numerous experimental tests were done by SAC (1996), (Noel and Uang, 1996) and (Uang, 1998) to investigate the effect of cyclic loading on connections strengthened with straight and triangular haunches. The results showed higher cyclic performance in the modified moment connections by welded haunches up to 0.025 rad. Figure 14 shows the specimen with straight haunch that is tested by Lee 2003.

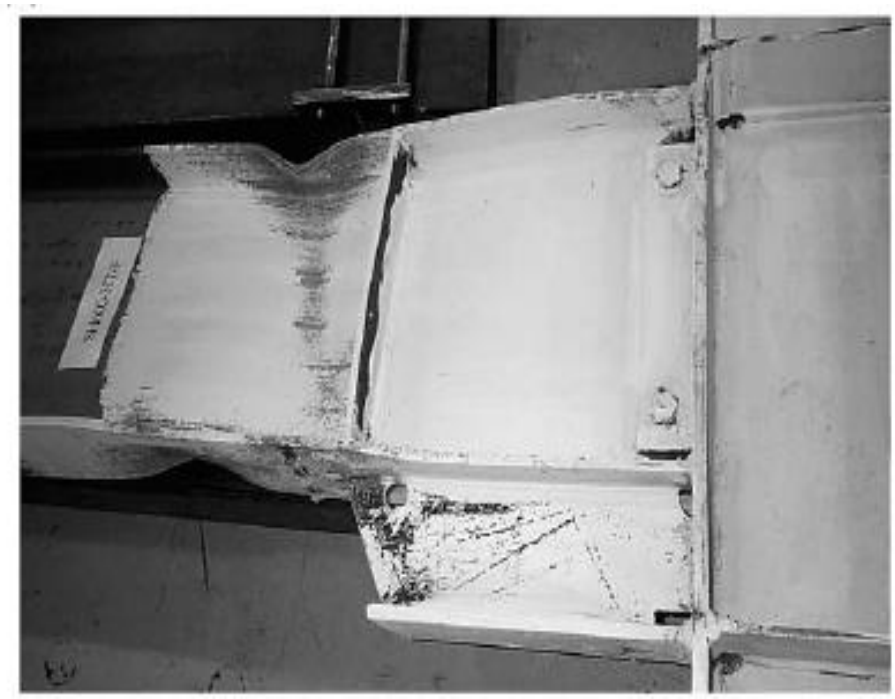

Figure 14: Plastic hinging of straight haunch specimen (Lee 2003)

2.2.1.4 Adding Bolted Brackets

The other method of strengthening is the addition of bolted bracket to the connection. The bolted brackets acted in a similar manner as the welded haunches with the benefit of fabrication since no welding was required and therefore, no fire protection was needed.

The high strength bolts are required to connect the bracket to the beam and column. Figure 15 illustrates an example to bolted brackets which connects the beam and column with high strength bolts. In 1997 and 1998 investigations by Kasai et al. have shown that this method is an effective modification method to provide high connection ductility.

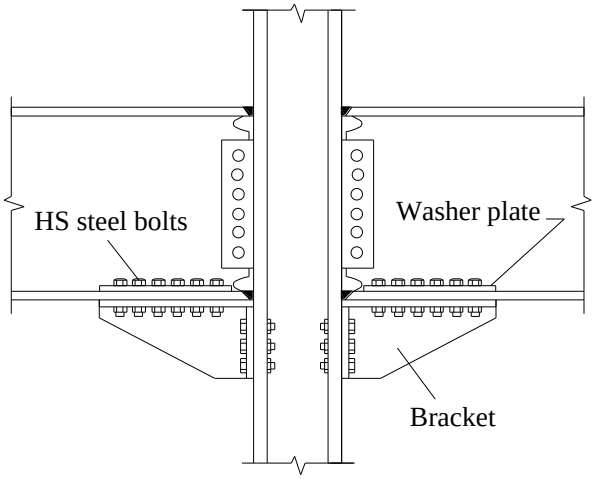

Figure 15: Bolted Bracket connection

There are several types of bolted brackets, such as, angle bracket connection, pipe bracket connection as shown in Figures 16 and 17.

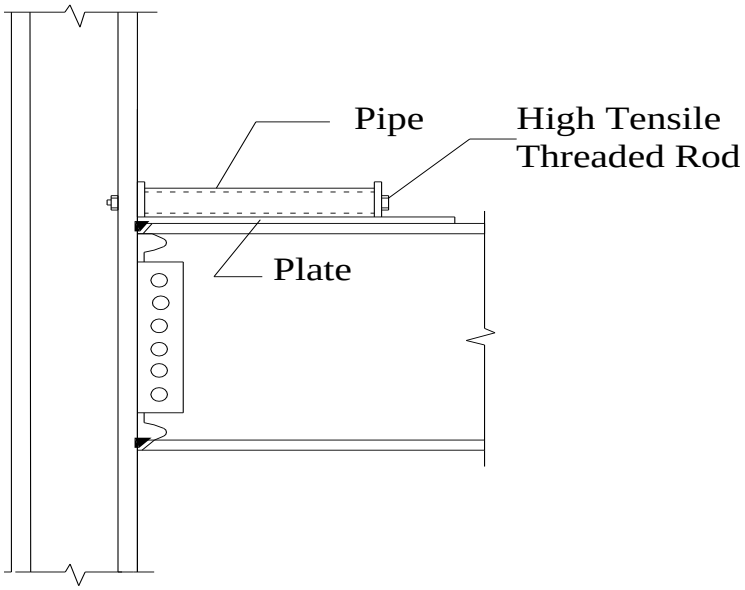

Figure 16: Angle bracket connection

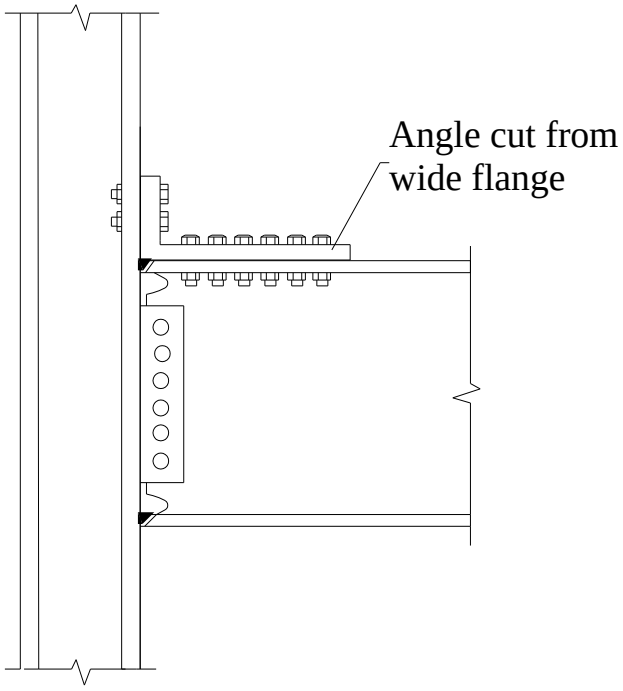

Figure 17: Pipe bracket connection

2.2.1.5 Adding Upstanding Ribs

Like haunches and brackets, rib plates are also used for strengthening the post-Northridge connection. Furthermore, it helps to reduce stresses at weld groove at

column face and beam flange, at the same time it moves the critical section far away from the beam flange and column face, simply connection region. Figure 18 is a type of upstanding rib that is used for strengthening the connection.

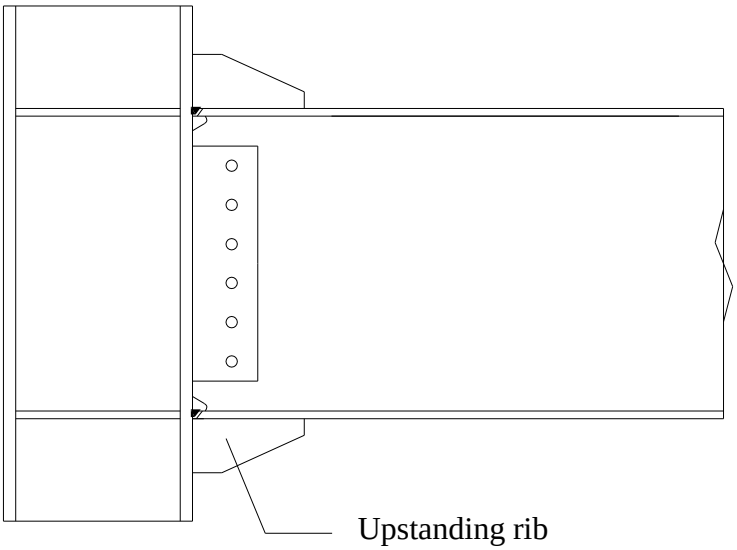

Figure 18: Strengthening of connection using upstanding ribs

This type of strengthening improved the performance of moment connections in cyclic loading (Engelhardt et al., 1995); (Anderson and Duan, 1998) and (Zekioglu et al., 1997). But this method of strengthening is not satisfactory in the case of beam early fractures as reported by Popov and Tsai, 1989 and Chen et al., 2005. On the other hand, the investigations showed that the single rib has more effective on the reduction of stress concentration in the weld area than the double spaced ribs.

2.2.1.6 Adding Lengthened Rib

One of the effective methods for strengthening is welding lengthened rib to the top and bottom of the beam flange centerline as it is shown in Figure 19 (Chen et al., 2003a and 2003b). The experimental test which was done by Chen et al at 2003 on the I-section column and at 2005 on the welded box section column had shown that

the connections strengthened with lengthened rib may pass 4 percent total rotation. In spite of the high performance of this modification, it would be very costly to remove the slab concrete near the column face and at the beam top flange of existing buildings to prepare enough space to add lengthened rib to the beam top flange.

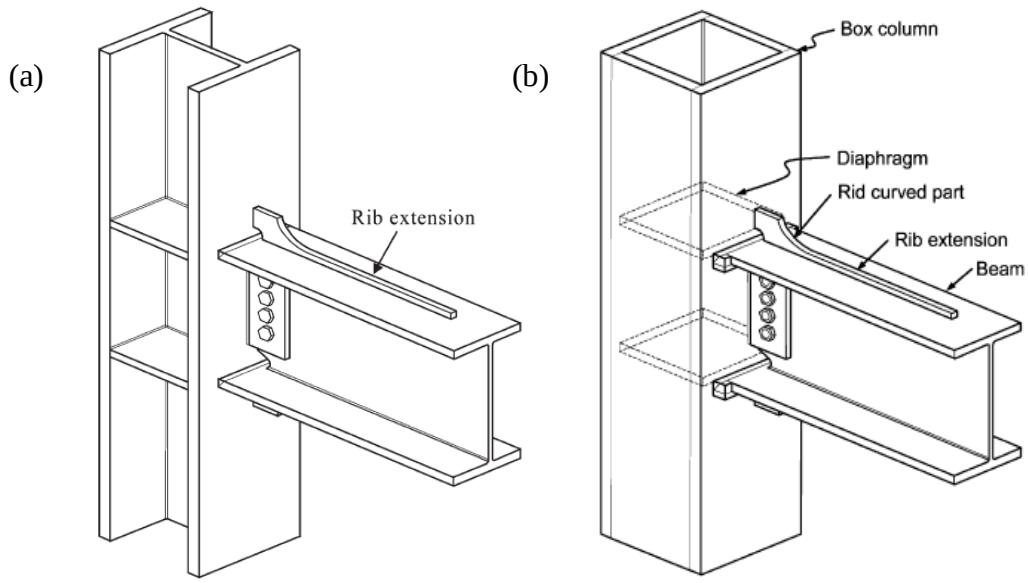

Figure 19: Lengthened flange rib strengthened connection: (a) With I-shape column (Chen, 2003a & 2003b); (b) With welded box-shape column (Chen et al., 2004)

2.2.1.7 Slit Damper

Saffari et al. (2013) designed and tested 8 different small types of slit dampers at the beam-column weld location to improve the ductility of the beam and strengthen the connection. Figures 20 and 21 show the finite element model and slit damper locations respectively. The finite element method analytical results had revealed that the slit dumpers would reduce the plastic strain and increase the strength of connection at the column-beam weld location causing the ductility of some specimens to reach 4.46 percent total rotation. The geometric properties and the force needed for slit damper yielding are same as those used by Chan and Albermani (2008).

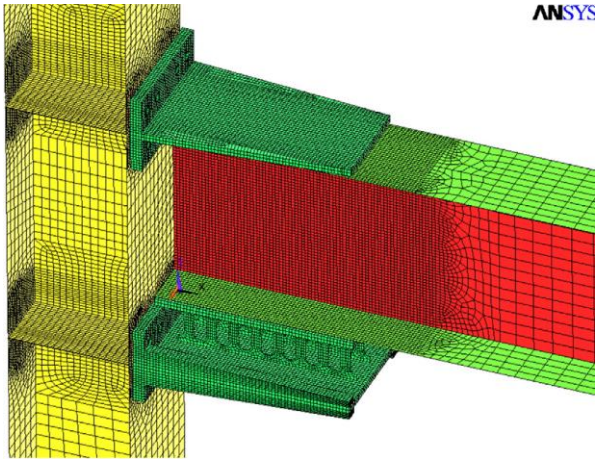

Figure 20: Finite element model of slit damper connection (Saffari et al., 2013)

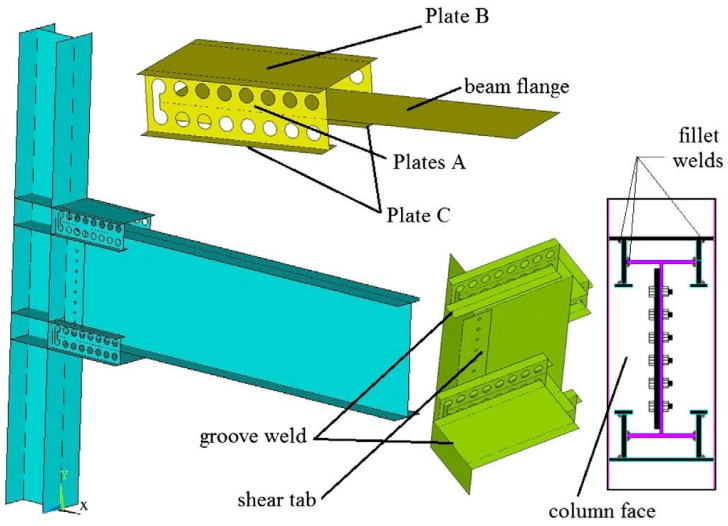

Figure 21: Slit damper parts and locations (Saffari et al., 2013)

2.2.2 Weakening of the Beam Section

The Reduced Beam Section (RBS) can be achieved in two methods by reducing the beam flange section or reducing the beam web section to gain enough ductility to achieve four percent total rotation. The following sections briefly explain various investigations conducted and their results in relation to RBS.

2.2.2.1 Reduced Beam Flange Section

The reduced beam flange section is used to improve the connections performance in similar manner as the reinforcement of connection. A typical reduced beam flange section is shown in Figure 22.

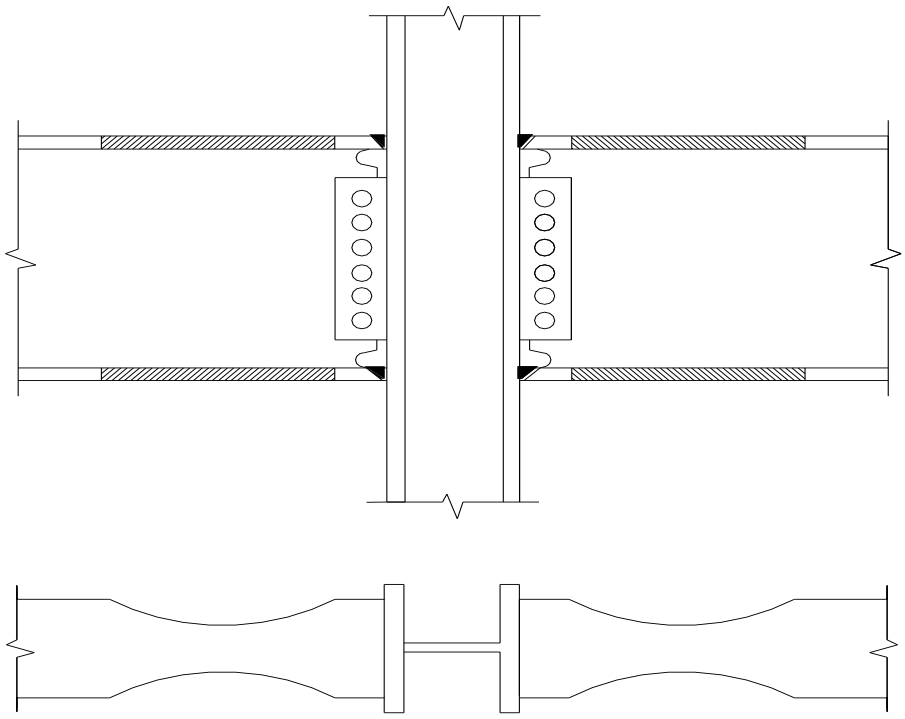

Figure 22: Reduced beam section (RBS) connection

Various investigations were done by Chen (1996 and 2001), Engelhardt (1996) and Uang (2000) to find the effect of reduced beam flange section on the beam to column connection with and without considering the concrete slab effect. The outcome from these experimental tests indicated that reduced beam flange approach gives results similar to those of the reinforcement method and in both methods plastic hinge was shifted away from the CJP at the column face. Figure 23 shows various types of reduced beam flange section.

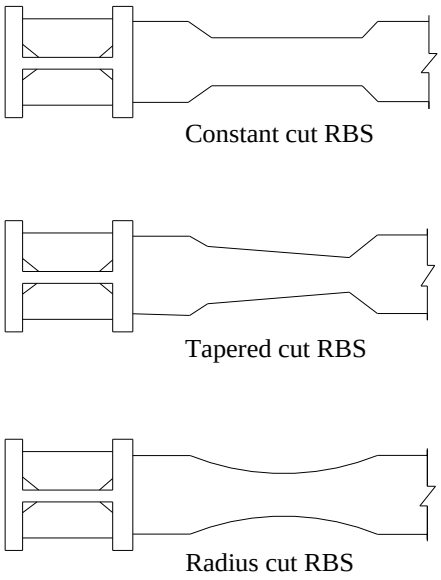

Figure 23: Various types of RBS connection

Despite of the acceptable performance of reduced beam flange section, it would be very costly to remove the slab concrete and to cut the top flange in existing buildings.

On the other hand, lateral torsional buckling is another problem which may happen and cause instability of the beam. However, before the lateral torsional buckling the RBS often experiences local buckling of web and after the lateral torsional buckling and it may have flange local buckling (Naeim, 2001).

2.2.2.2 Slotted Web Connection

In 1998 Allen tested and introduced design of slotted web connections. Majority of this type of connection is very similar to pre-Northridge connection as it is illustrated in AISC-LRFD Manual of Steel Construction Design (1995). The general form of slotted web connection can be seen in Figure 24. A new configuration of this type of web connections was tested by Maleki and Tabbakhha (2012) (Figure 25). They aim

to improve the energy dissipation at the connection to reduce the concentration of stresses at the CJP by changing the slotted web connection to the Slotted-Web–Reduced-Flange. In some cases the results show better performance than RBS.

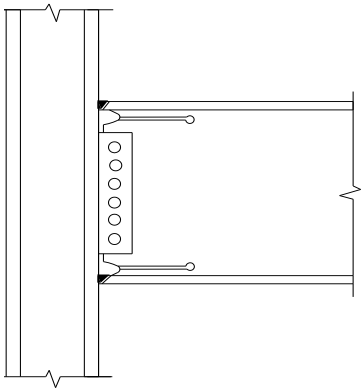

Figure 24: Proprietary Slotted Web Connection (Allen 1998)

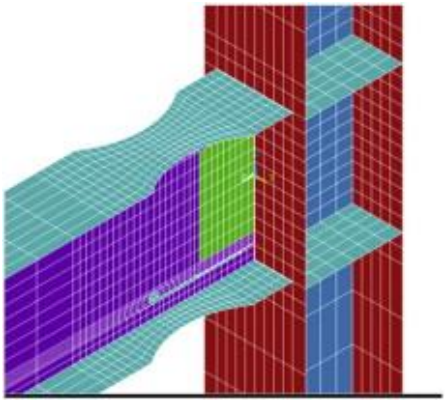

Figure 25: Three-dimensional slotted web connection FEM model (Maleki and Tabbakhha, 2012)

2.2.2.3 Wedge Design Connection

Wilkinson used the Wedge Design Connections in 2006. Part of web and flange of the beam removed and the flange re attached to the beam as shown in Figure 26.

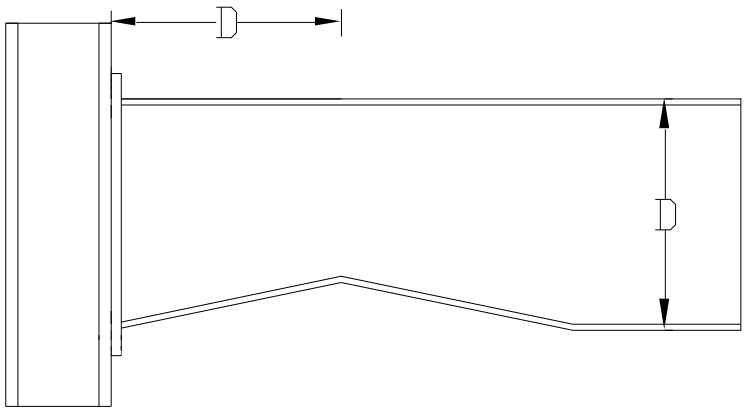

Figure 26: Geometry of the wedge detail (Wilkinson, 2006)

By removing the wedge from the beam Wilkinson managed to move the plastic hinge to a distance equal to beam depth (D) which is far from the beam to column weld location. The results showed that the shallow beam specimens easily achieved minimum 3 percent plastic rotation.

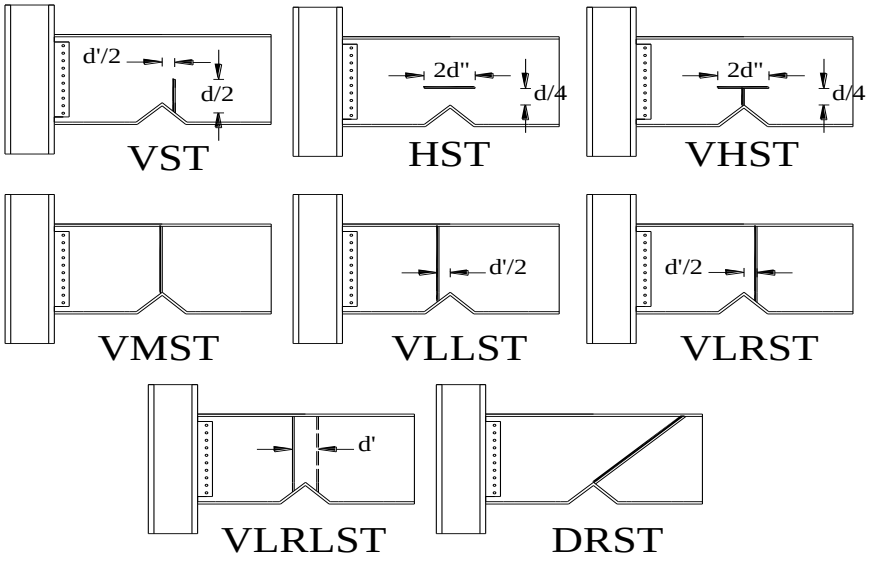

Figure 27: Different stiffener configurations used for specimen SAC7-WA35.

Figure 27 shows the modifications suggested to wedge connection by Hedayat and Celikag (2010) to control the beam web buckling by using stiffener in the web to enhance 4 percent total rotation in deep and moderate beams sections.

2.2.2.4 Double Wedge Specimens

The other method which is suggested by Hedayat and Celikag is double wedge specimens. In this method they improved the beam ductility and plastic moment capacity by making 2 plastic hinges at a distance equal to one half of the beam depth (0.5×D) and beam depth (1×D) from the beam to column weld location. Figure 28 shows different types of double wedge specimens that is designed and used by Hedayat and Celikag investigation.

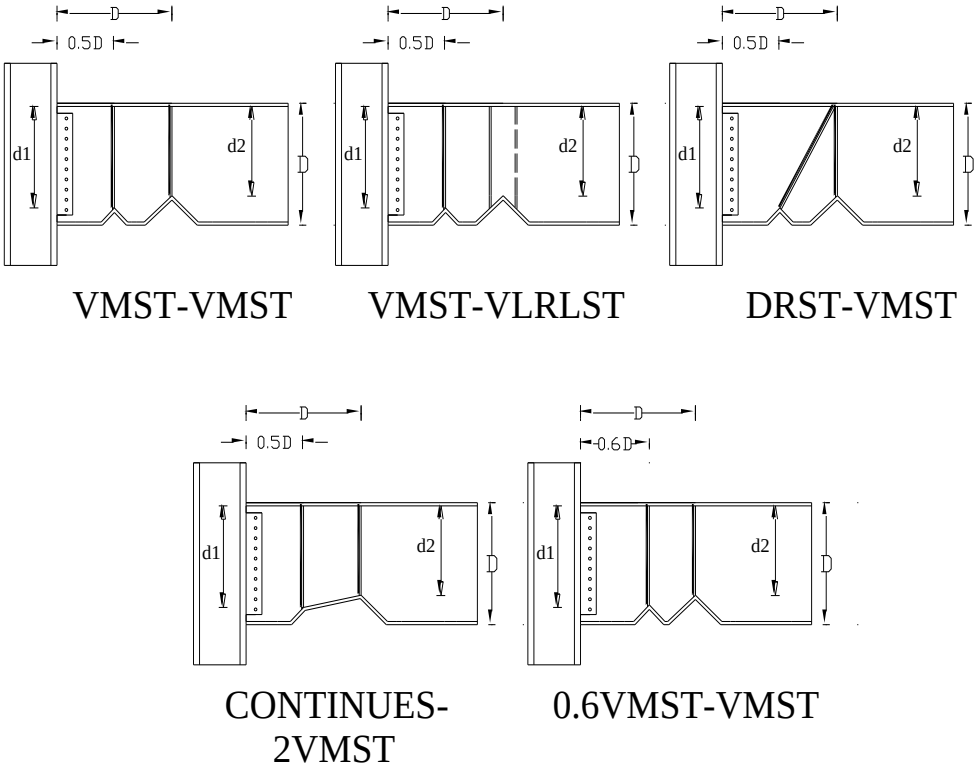

Figure 28: Geometry of double wedge design specimens (Hedayat and Celikag, 2010)

2.2.2.5 Circular Void Reduced Beam Web (RBW) Connections

Ascheheim presented a new method in reduced beam web connection at 2000; the new method was conducted by reducing the number of circular sections from the beam web as shown in Figure 29. Aschheim has selected the distances between the

circles and the sizes of the circles to dissipate the shear yielding through the beam span. In this way he shifted the plastic hinge away from the weld location. The experimental tests were conducted on 5 US patent sections (W21×68 Grade 50) under cyclic loading. The results of the investigation have shown that the specimen manage to achieve 6 percent of inter story drift (Ascheheim, 2000).

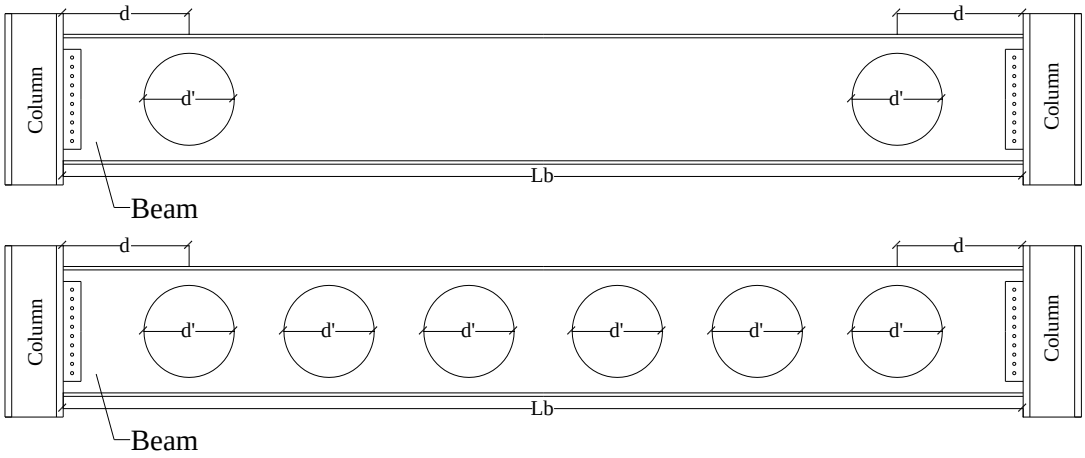

Figure 29: RBW connection proposed by Aschheim (2000)

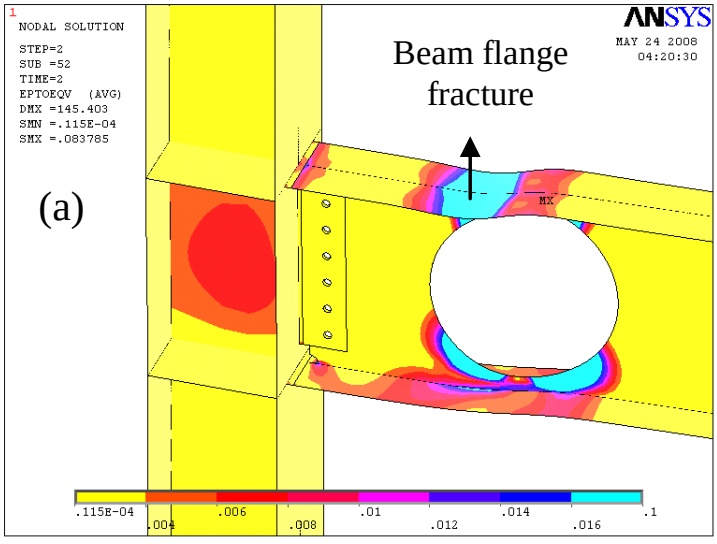

(a)

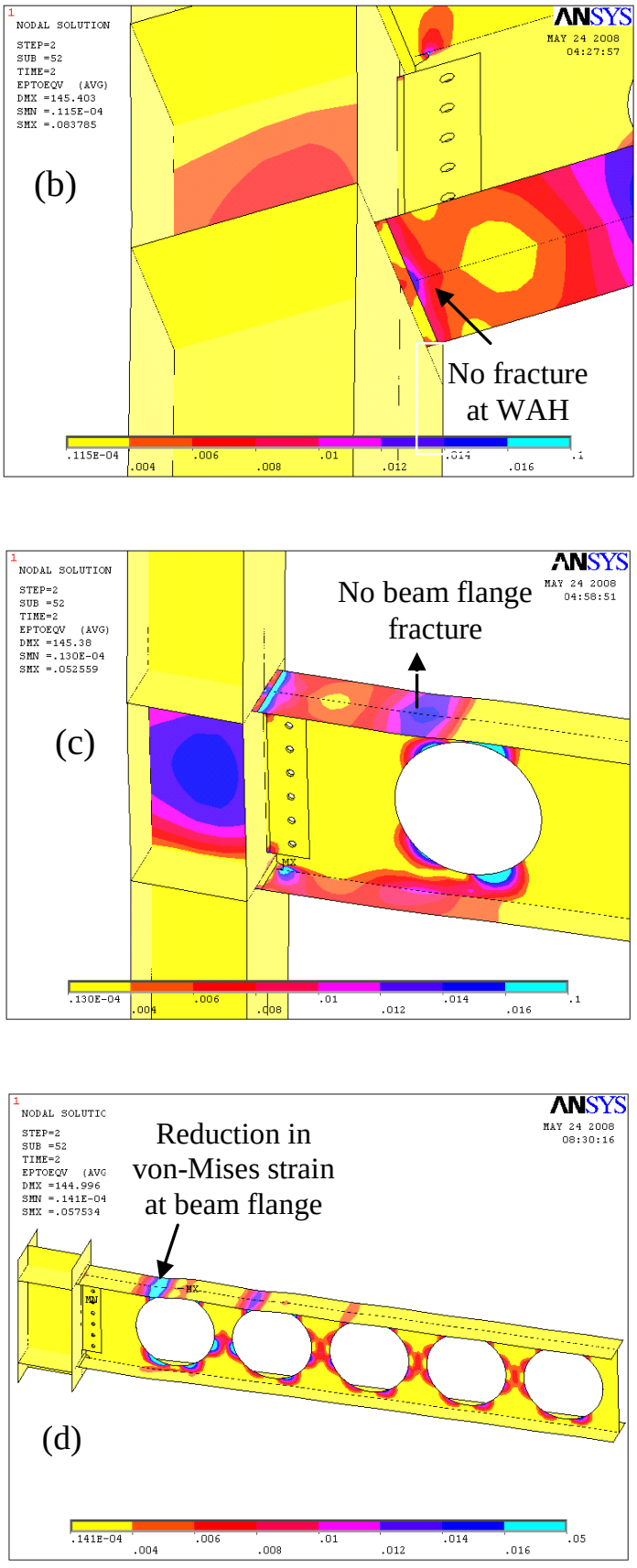

Figure 30: The behavior of typical circular RBW connections (Hedayat and Celikag, 2010)

2.2.2.6 Longitudinal Void Configuration

Figure 29 shows the different type of reduction in the beam web that is investigated by Hedayat and Celikag (2009) the results have shown the big voids need to reduce the stress in the beam column weld location to conduct enough ductility to achieve 4 percent total rotation. Despite of stress reduction at connection, the premature fracture in the voids was the disadvantage of this type of configuration. Hedayat and Celikag designed the longitudinal voids and strengthen the web by using stiffener and box as it is shown in Figure 31. The FEM results showed that specimens easily passed 4 percent total rotation.

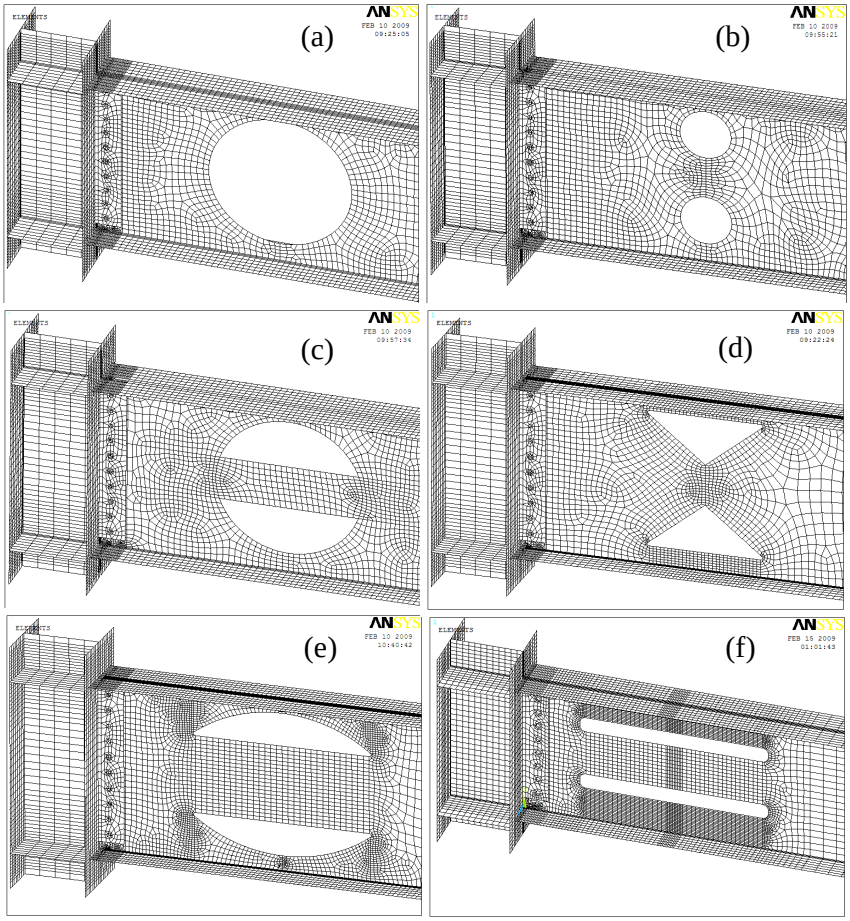

Figure 31: The types of BEC's Investigated (Hedayat and Celikag, 2009)

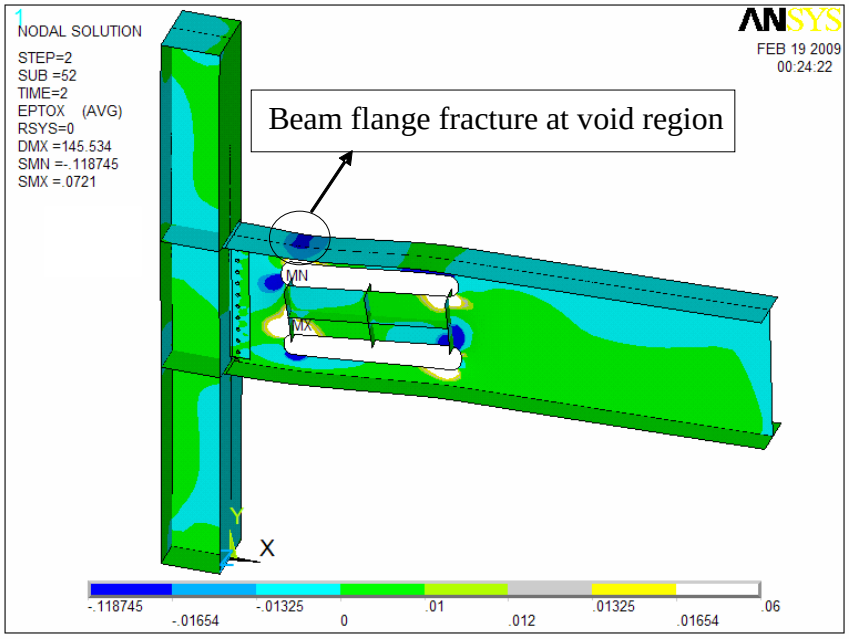

Figure 32: Premature fracture at the starting point of void (Hedayat and Celikag, 2009)

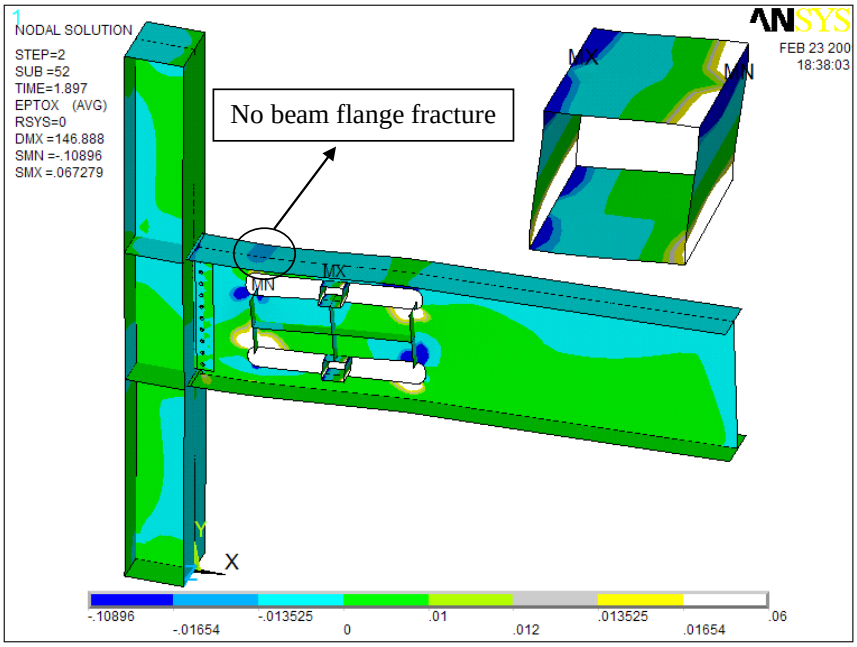

Figure 33: Modified reduced beam web to control the fracture at starting point of the void (Hedayat and Celikag, 2009)

2.2.2.7 Multi Longitudinal Voids Configuration

Multi Longitudinal Voids (MLV) configuration is investigated in this thesis to suggest a new design method in Reducing the Beam Web (RBW) to achieve minimum 4 percent total rotation while the modification is practical and cost effective for application to existing buildings. In this configuration 2 pair of longitudinal voids would be open in the beam web to improve the energy dissipation along the beam web to achieve enough ductility and strength for the connection (4 percent total rotation) while reducing the shear stress in the beam-column weld location at CJP by moving plastic hinge away from weld location at the column face. Figure 34 shows the multi longitudinal voids in beam web.

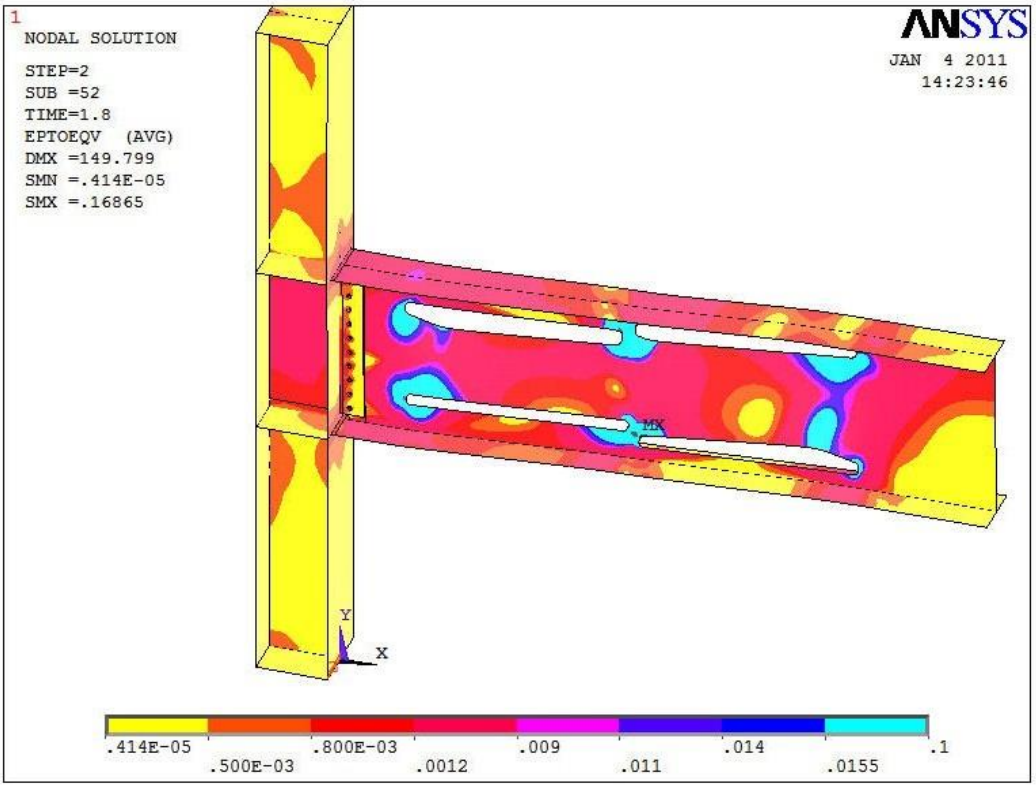

Figure 34: Multi longitudinal voids configuration

Chapter 3

METHODOLOGY

3.1 Finite Element Method

ANSYS (2007) finite element program was used to model the SAC3, SAC5 and SAC7 post-Northridge connections, which are good representatives of small, medium and large size connections and previously tested by Lee and Stojadinovic (2001). The details of these connections are given in Table 1. The length of the beam ($L_b/2$) and the column for all these specimens were 3429 mm and 3658 mm respectively. 0.3 and 200 kN/mm^2 are taken as the poisson's ratio and modulus of elasticity respectively**.** Other geometric parameters and all the other material properties of these specimens are summarized in Tables 1 and 2. The proposed beam end configuration with different values of design parameters was then applied to all these post-Northridge connections to create modified post-Northridge specimens.

After Northridge earthquake, Miller (1998) inspected more than 100 damaged buildings and also experimental tests were conducted by the SAC group (e.g. Lee and Stojadinovic (2001)) on the pre and the post-Northridge connections. The results showed that, the failure of the connection was not due to the failure of bolts until the rapture of the CJP.

Table 1: Geometric parameters of SAC specimens

specimen	Beam Section	Column Section	Shear tab (mm)	No. of A325 SC Bolts (mm)	Continuity plate (mm)	Weld type and size (mm)	
						Beam flange	shear tab
SAC3	W24x68	W14x120	457x127x9.5	6Φ22	305x127x16	CJP, root opening= 9 mm, bevel angle=30◦ and E70TG-K2	Fillet, 8mm, E70T-7
SAC5	W30x99	W14x176	610x127x12.7	8Φ25	305x127x19		
SAC7	W36x150	W14x257	762x127x15.9	10Φ25	305x152x25.4		

Table 2: Material properties of the SAC specimens (MPa)

Specimen F_y/F_u	Beam		Column		Shear tab	Continuity plate
	Flange	Web	Flange	Web		
SAC3	315.2/468.1	340.9/480.6	319.4/469.4	345.8/475.0	323.6/490.3	358.3/509.7
SAC5	355.5/484.7	382.6/497.2	360.4/511.1	356.2/500.3	288.9/446.5	302.1/444.4
SAC7	290.3/441.7	327.1/447.2	335.4/490.3	306.9/475.7	358.3/509.7	310.4/475.7

Therefore, in order to achieve a realistic finite element model, shear tab, bolt holes and interaction between the shear tab and the beam web were properly modeled but the bolts were not exactly modeled. Shell elements were used for the finite element modeling of both welds and base metals and their material properties were individually defined. One-layer four-node shell elements, SHELL43, were used to model weld, continuity plates, stiffener plates for column and shear tab. Multi-layer eight-node shell elements, SHELL181, were used to model the beam plates. Each node of these elements has six degrees of freedom and they are capable to have large deflection, plasticity and large strain. In this study each element of SHELL181 was divided into five layers across the thickness, based on the finite element study done by Gilton and Uang (2002).

According to the recommendations by ANSYS program, both modified and non-modified specimens were subjected to a mesh sensitivity study to determine their appropriate mesh density. Furthermore, the analytical results were also compared with the experimental results (Lee and Stojadinovic, 2001). The finite element mesh for the connection with multi longitudinal voids is shown in Figure 35. In order to capture the local buckling of the beam flange and web accurately at the voids area a very fine mesh size was used for the beam flange and web area. The number of elements for specimens (SAC3, SAC5 and SAC7) in average was 27,000. Around 30 to 50 percent of these elements were due to the size of the voids located at the beam web.

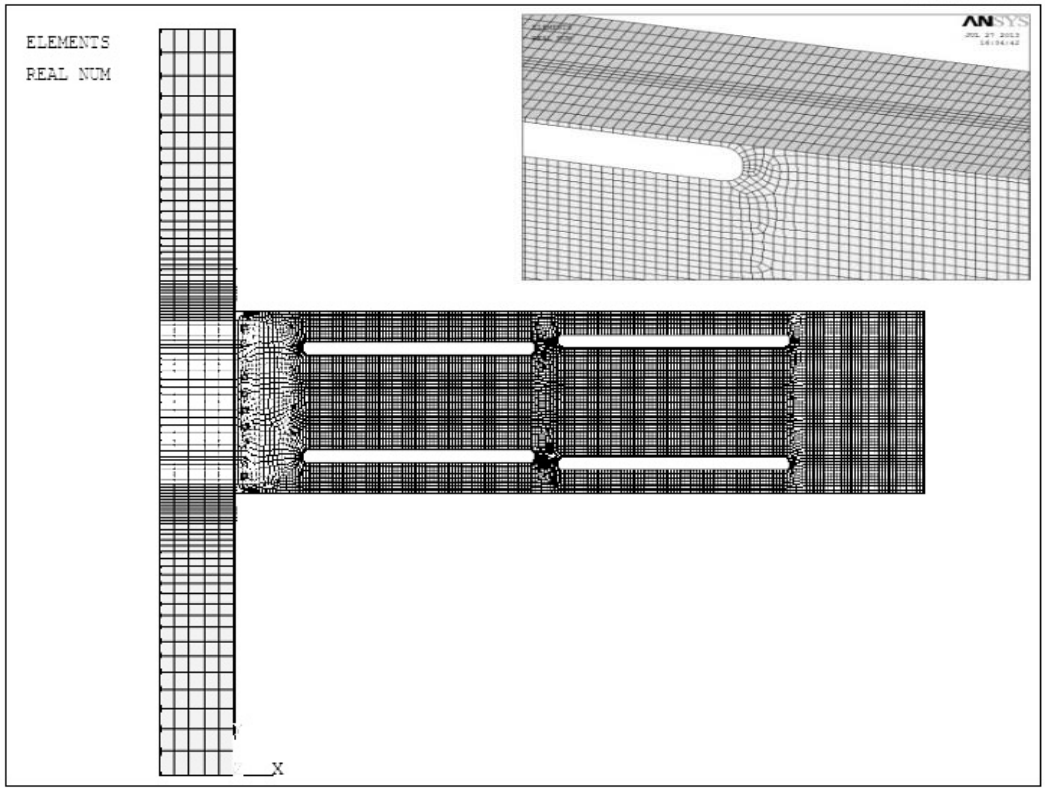

Figure 35: Typical finite element mesh of a RBW with multi longitudinal voids

The flow rule and the yielding criteria of Von-Mises stress was used to obtain the plastic behavior for material nonlinear analysis. For monotonic analysis isotropic hardening and for cyclic analysis kinematic hardening was assumed as used by Mao et al. (2001) Ricles et al. (2003) respectively. A bilinear material response with a post yielding stiffness equal to 4 percent of the modulus of elasticity of steel was used for the base metals in accordance with the material properties given by Lee and Stojadinovic (2001). The material property given by Mao et al. (2001) and Ricles et al. (2003) was used to obtain the multi-linear material response for weld metals (Figure 37). For analysis with monotonic loading, a vertical load was applied at the free end of the beam, in one direction only, until the column web centre total rotation was reached to 4 percent. On the other hand, for analysis with cyclic loading, the load history recommended by FEMA350 (2000) was used. Deformations in the out-

of-plane direction (direction normal to the beam web) may not happen when the specimen is subject to loads in the vertical direction (direction parallel to the beam web). Out-of-plane deformations or buckling may occur when the beam is subject to vertical loads only. However, buckling may occur due to instability in the model, which can be obtained by analyzing an imperfect model. In this study, the imperfect model was determined through separate buckling analysis to obtain the buckling mode shapes and then applying the results to the SAC group original perfect geometry (Kim et al., 2000).

In order to verify the validity of the numerical research, Hedayat and Celikag (2009, 2010) prepared finite element models for the specimens SAC3, SAC5 and SAC7 of the experimental study conducted by Lee and Stojadinovic (2001). The numerical results agreed suitably with the experimental ones as shows in Figure 36.

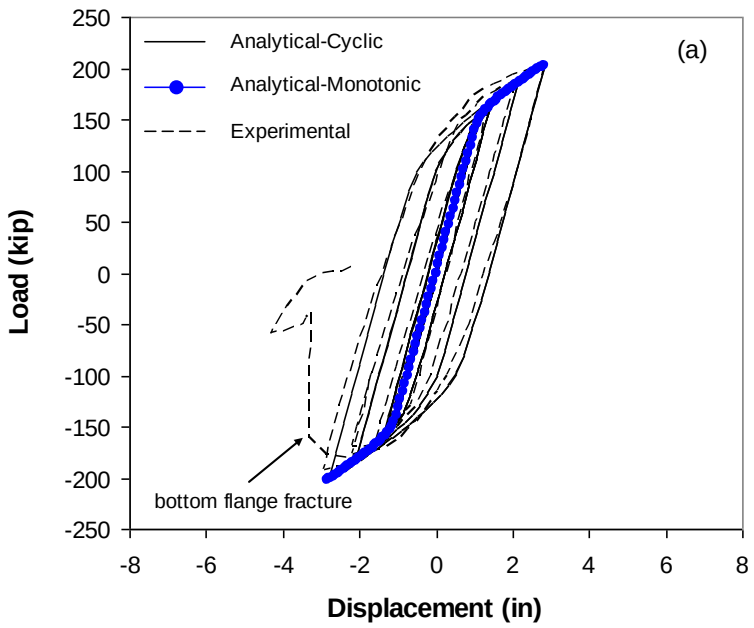

(a)

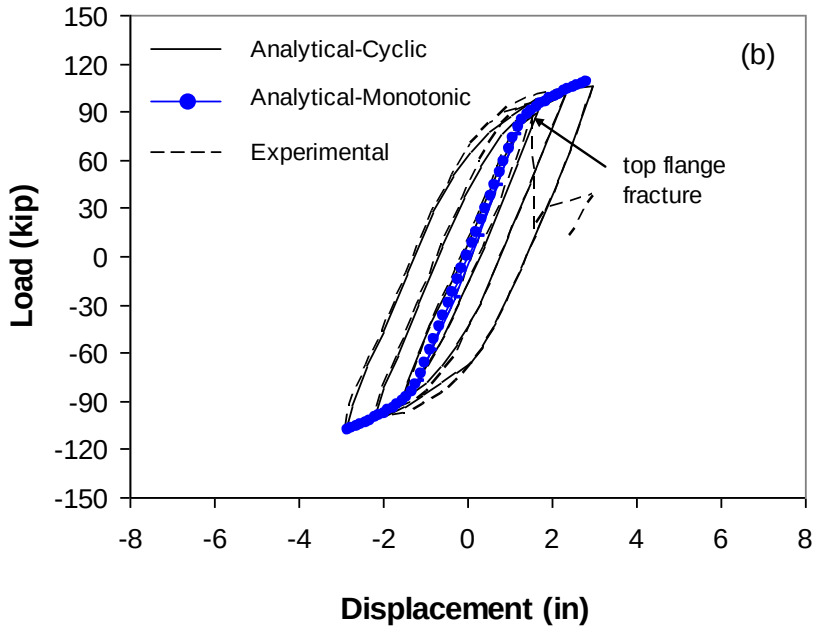

(b)

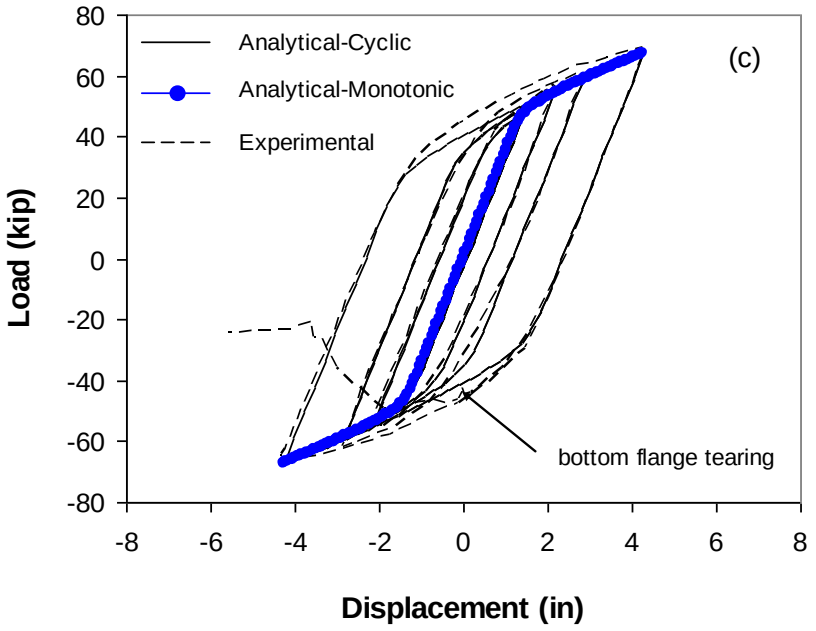

(c)

Figure 36: Beam tip load versus beam tip displacement of analytical and experimental results for pre-tested specimens by Lee et al. (2000): (a) SAC7; (b) SAC5; (c) SAC3

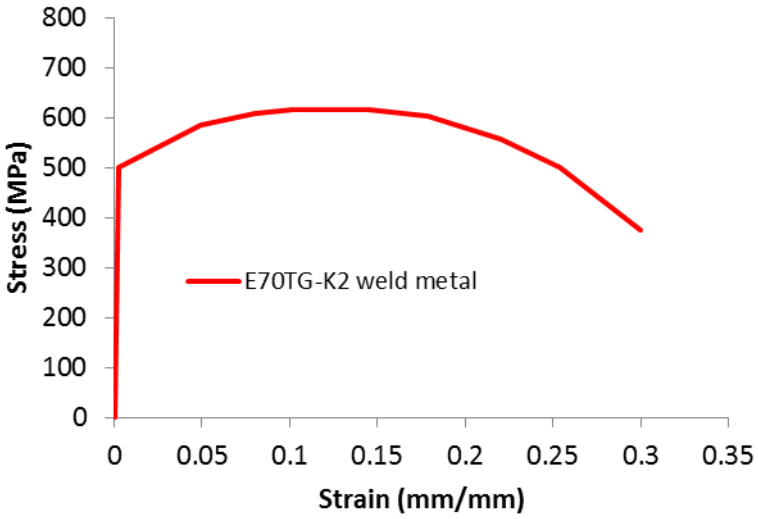

Figure 37: Stress-strain relationship used for the weld metal (Mao et al., (2001) and Ricles et al. (2003))

In this study, in order to validate the previous research by Hedayat and Celikag (2009) the 3 post-Northridge non modified connections (SAC3, SAC5 and SAC7) and 26 modified connections with single pair of voids were modeled. Then 144 modified SAC3, SAC5 and SAC7 connections with two pairs of voids were modeled. The details about the total of 173 models are given in Tables 3 to 5.

Table 3: SAC 7 parameters and dimensions

	Beam	Column	Unitless Parameters			L (mm)	L_b (mm)	L_c (mm)	First pair of voids dimensions						Second pair of voids dimensions					
			α	β	γ				a (mm)	b (mm)	D_v (mm)	L_v (mm)	r_v (mm)	Sc (mm)	a (mm)	b (mm)	Dv (mm)	Lv (mm)	rv (mm)	Sc (mm)
Single Void SAC7	W36X150	W14X257				7216,1	6800	3657,6												
				4		7216,1	6800	3657,6	465	171,5	40	1140	10	351,86						
				3		7216,1	6800	3657,6	465	161,5	50	1140	15	356,86						
				2,5		7216,1	6800	3657,6	465	137,5	55	1140	20	361,86						
				2		7216,1	6800	3657,6	465	130	65	1140	25	366,86						
				1,5		7216,1	6800	3657,6	465	120	80	1140	30	371,86						
				1		7216,1	6800	3657,6	465	100	100	1140	40	381,86						
				0,75		7216,1	6800	3657,6	465	86,25	115	1140	45	386,86						
				0,5		7216,1	6800	3657,6	465	65	130	1140	55	396,86						
				0,25		7216,1	6800	3657,6	465	40	160	1140	70	411,86						

Table 3: SAC 7 parameters and dimensions (continued)

	Beam	Column	Unitless Parameters			L (mm)	L_b (mm)	L_c (mm)	First pair of voids dimensions						Second pair of voids dimensions					
			α	β	γ				a (mm)	b (mm)	D_v (mm)	L_v (mm)	r_v (mm)	Sc (mm)	a (mm)	b (mm)	Dv (mm)	Lv (mm)	rv (mm)	Sc (mm)
Multi Logitudinal Voids SAC7	W36X150	W14X257	2	0.25	0.1	7216.1	6800	3657.6	465	130	65	1140	25	366.86	684.6	36.625	65	1140	25	366.86
			2	0.5	0.1	7216.1	6800	3657.6	465	130	65	1140	25	366.86	611.4	73.25	65	1140	25	366.86
			2	0.75	0.1	7216.1	6800	3657.6	465	130	65	1140	25	366.86	538.2	109.88	65	1140	25	366.86
			2	1	0.1	7216.1	6800	3657.6	465	130	65	1140	25	366.86	465	146.5	65	1140	25	366.86
			2	0.25	0.15	7216.1	6800	3657.6	465	130	65	1140	25	366.86	684.6	36.625	65	1140	25	366.86
			2	0.5	0.15	7216.1	6800	3657.6	465	130	65	1140	25	366.86	611.4	73.25	65	1140	25	366.86
			2	0.75	0.15	7216.1	6800	3657.6	465	130	65	1140	25	366.86	538.2	109.88	65	1140	25	366.86
			2	1	0.15	7216.1	6800	3657.6	465	130	65	1140	25	366.86	465	146.5	65	1140	25	366.86
			2	0.25	0.2	7216.1	6800	3657.6	465	130	65	1140	25	366.86	684.6	36.625	65	1140	25	366.86
			2	0.5	0.2	7216.1	6800	3657.6	465	130	65	1140	25	366.86	611.4	73.25	65	1140	25	366.86
			2	0.75	0.2	7216.1	6800	3657.6	465	130	65	1140	25	366.86	538.2	109.88	65	1140	25	366.86
			2	1	0.2	7216.1	6800	3657.6	465	130	65	1140	25	366.86	465	146.5	65	1140	25	366.86
			2	0.25	0.25	7216.1	6800	3657.6	465	130	65	1140	25	366.86	684.6	36.625	65	1140	25	366.86
			2	0.5	0.25	7216.1	6800	3657.6	465	130	65	1140	25	366.86	611.4	73.25	65	1140	25	366.86
			2	0.75	0.25	7216.1	6800	3657.6	465	130	65	1140	25	366.86	538.2	109.88	65	1140	25	366.86
			2	1	0.25	7216.1	6800	3657.6	465	130	65	1140	25	366.86	465	146.5	65	1140	25	366.86

Table 3: SAC 7 parameters and dimensions (continued)

	Beam	Column	Unitless Parameters			L (mm)	L_b (mm)	L_c (mm)	First pair of voids dimensions						Second pair of voids dimensions					
			α	β	γ				a (mm)	b (mm)	D_v (mm)	L_v (mm)	r_v (mm)	Sc (mm)	a (mm)	b (mm)	Dv (mm)	Lv (mm)	rv (mm)	Sc (mm)
Multi Logitudinal Voids SAC7	W36X150	W14X257	3	0.25	0.1	7216.1	6800	3657.6	465	161.5	50	1140	20	361.86	707.2	40.4	50	1140	15	356.86
			3	0.5	0.1	7216.1	6800	3657.6	465	161.5	50	1140	20	361.86	626.4	80.8	50	1140	15	356.86
			3	0.75	0.1	7216.1	6800	3657.6	465	161.5	50	1140	20	361.86	545.8	121.1	50	1140	15	356.86
			3	1	0.1	7216.1	6800	3657.6	465	161.5	50	1140	20	361.86	465	161.5	50	1140	15	356.86
			3	0.25	0.15	7216.1	6800	3657.6	465	161.5	50	1140	20	361.86	707.2	40.4	50	1140	15	356.86
			3	0.5	0.15	7216.1	6800	3657.6	465	161.5	50	1140	20	361.86	626.4	80.8	50	1140	15	356.86
			3	0.75	0.15	7216.1	6800	3657.6	465	161.5	50	1140	20	361.86	545.8	121.1	50	1140	15	356.86
			3	1	0.15	7216.1	6800	3657.6	465	161.5	50	1140	20	361.86	465	161.5	50	1140	15	356.86
			3	0.25	0.2	7216.1	6800	3657.6	465	161.5	50	1140	20	361.86	707.2	40.4	50	1140	15	356.86
			3	0.5	0.2	7216.1	6800	3657.6	465	161.5	50	1140	20	361.86	626.4	80.8	50	1140	15	356.86
			3	0.75	0.2	7216.1	6800	3657.6	465	161.5	50	1140	20	361.86	545.8	121.1	50	1140	15	356.86
			3	1	0.2	7216.1	6800	3657.6	465	161.5	50	1140	20	361.86	465	161.5	50	1140	15	356.86
			3	0.25	0.25	7216.1	6800	3657.6	465	161.5	50	1140	20	361.86	707.2	40.4	50	1140	15	356.86
			3	0.5	0.25	7216.1	6800	3657.6	465	161.5	50	1140	20	361.86	626.4	80.8	50	1140	15	356.86
			3	0.75	0.25	7216.1	6800	3657.6	465	161.5	50	1140	20	361.86	545.8	121.1	50	1140	15	356.86
			3	1	0.25	7216.1	6800	3657.6	465	161.5	50	1140	20	361.86	465	161.5	50	1140	15	356.86

Table 3: SAC 7 parameters and dimensions (continued)

	Beam	Column	Unitless Parameters			L (mm)	L_b (mm)	L_c (mm)	First pair of voids dimensions						Second pair of voids dimensions					
			α	β	γ				a (mm)	b (mm)	D_v (mm)	L_v (mm)	r_v (mm)	Sc (mm)	a (mm)	b (mm)	Dv (mm)	Lv (mm)	rv (mm)	Sc (mm)
Multi Logitudinal Voids SAC7	W36X150	W14X257	4	0.25	0.1	7216.1	6800	3657.6	465	171.5	40	1140	10	351.86	722.2	42.9	40	1140	10	351.86
			4	0.5	0.1	7216.1	6800	3657.6	465	171.5	40	1140	10	351.86	636.4	85.8	40	1140	10	351.86
			4	0.75	0.1	7216.1	6800	3657.6	465	171.5	40	1140	10	351.86	550.8	128.6	40	1140	10	351.86
			4	1	0.1	7216.1	6800	3657.6	465	171.5	40	1140	10	351.86	465	171.5	40	1140	10	351.86
			4	0.25	0.15	7216.1	6800	3657.6	465	171.5	40	1140	10	351.86	722.2	42.9	40	1140	10	351.86
			4	0.5	0.15	7216.1	6800	3657.6	465	171.5	40	1140	10	351.86	636.4	85.8	40	1140	10	351.86
			4	0.75	0.15	7216.1	6800	3657.6	465	171.5	40	1140	10	351.86	550.8	128.6	40	1140	10	351.86
			4	1	0.15	7216.1	6800	3657.6	465	171.5	40	1140	10	351.86	465	171.5	40	1140	10	351.86
			4	0.25	0.2	7216.1	6800	3657.6	465	171.5	40	1140	10	351.86	722.2	42.9	40	1140	10	351.86
			4	0.5	0.2	7216.1	6800	3657.6	465	171.5	40	1140	10	351.86	636.4	85.8	40	1140	10	351.86
			4	0.75	0.2	7216.1	6800	3657.6	465	171.5	40	1140	10	351.86	550.8	128.6	40	1140	10	351.86
			4	1	0.2	7216.1	6800	3657.6	465	171.5	40	1140	10	351.86	465	171.5	40	1140	10	351.86
			4	0.25	0.25	7216.1	6800	3657.6	465	171.5	40	1140	10	351.86	722.2	42.9	40	1140	10	351.86
			4	0.5	0.25	7216.1	6800	3657.6	465	171.5	40	1140	10	351.86	636.4	85.8	40	1140	10	351.86
			4	0.75	0.25	7216.1	6800	3657.6	465	171.5	40	1140	10	351.86	550.8	128.6	40	1140	10	351.86
			4	1	0.25	7216.1	6800	3657.6	465	171.5	40	1140	10	351.86	465	171.5	40	1140	10	351.86

Table 4: SAC 5 parameters and dimensions

	Beam	Column	Unitless Parameters			L (mm)	L_b (mm)	L_c (mm)	First pair of voids dimensions						Second pair of voids dimensions					
			α	β	γ				a (mm)	b (mm)	D_v (mm)	L_v (mm)	r_v (mm)	Sc (mm)	a (mm)	b (mm)	Dv (mm)	Lv (mm)	rv (mm)	Sc (mm)
Single Void SAC5	W 30*99	W 14*176				7193.8	6807	3660												
				4		7193.8	6807	3660	300	178	40	940	10	293.11						
				3		7193.8	6807	3660	300	168	50	940	15	298.11						
				2.5		7193.8	6807	3660	300	158	60	940	20	303.11						
				2		7193.8	6807	3660	300	148	70	940	25	308.11						
				1.5		7193.8	6807	3660	300	133	85	940	30	313.11						
				1		7193.8	6807	3660	300	113	105	940	45	328.11						
				0.75		7193.8	6807	3660	300	98	120	940	50	333.11						
				0.5		7193.8	6807	3660	300	78	140	940	60	343.11						
				0.25		7193.8	6807	3660	300	48	170	940	75	358.11						

Table 4: SAC 5 parameters and dimensions (continued)

	Beam	Column	Unitless Parameters			L (mm)	L_b (mm)	L_c (mm)	First pair of voids dimensions						Second pair of voids dimensions					
			α	β	γ				a (mm)	b (mm)	D_v (mm)	L_v (mm)	r_v (mm)	Sc (mm)	a (mm)	b (mm)	Dv (mm)	Lv (mm)	rv (mm)	Sc (mm)
Multi Logitudinal Voids SAC5	W 30*99	W 14*176	2	0.25	0.1	7193.8	6807	3660	300	148	70	940	25	308.11	522	37	70	940	25	308.11
			2	0.5	0.1	7193.8	6807	3660	300	148	70	940	25	308.11	448	74	70	940	25	308.11
			2	0.75	0.1	7193.8	6807	3660	300	148	70	940	25	308.11	374	111	70	940	25	308.11
			2	1	0.1	7193.8	6807	3660	300	148	70	940	25	308.11	300	148	70	940	25	308.11
			2	0.25	0.15	7193.8	6807	3660	300	148	70	940	25	308.11	522	37	70	940	25	308.11
			2	0.5	0.15	7193.8	6807	3660	300	148	70	940	25	308.11	448	74	70	940	25	308.11
			2	0.75	0.15	7193.8	6807	3660	300	148	70	940	25	308.11	374	111	70	940	25	308.11
			2	1	0.15	7193.8	6807	3660	300	148	70	940	25	308.11	300	148	70	940	25	308.11
			2	0.25	0.2	7193.8	6807	3660	300	148	70	940	25	308.11	522	37	70	940	25	308.11
			2	0.5	0.2	7193.8	6807	3660	300	148	70	940	25	308.11	448	74	70	940	25	308.11
			2	0.75	0.2	7193.8	6807	3660	300	148	70	940	25	308.11	374	111	70	940	25	308.11
			2	1	0.2	7193.8	6807	3660	300	148	70	940	25	308.11	300	148	70	940	25	308.11
			2	0.25	0.25	7193.8	6807	3660	300	148	70	940	25	308.11	522	37	70	940	25	308.11
			2	0.5	0.25	7193.8	6807	3660	300	148	70	940	25	308.11	448	74	70	940	25	308.11
			2	0.75	0.25	7193.8	6807	3660	300	148	70	940	25	308.11	374	111	70	940	25	308.11
			2	1	0.25	7193.8	6807	3660	300	148	70	940	25	308.11	300	148	70	940	25	308.11

Table 4: SAC 5 parameters and dimensions (continued)

	Beam	Column	Unitless Parameters			L (mm)	L_b (mm)	L_c (mm)	First pair of voids dimensions						Second pair of voids dimensions					
			α	β	γ				a (mm)	b (mm)	D_v (mm)	L_v (mm)	r_v (mm)	Sc (mm)	a (mm)	b (mm)	Dv (mm)	Lv (mm)	rv (mm)	Sc (mm)
Multi Logitudinal Voids SAC5	W 30*99	W 14*176	3	0.25	0.1	7193.8	6807	3660	300	168	50	940	15	298.11	552	42	50	940	15	298.11
			3	0.5	0.1	7193.8	6807	3660	300	168	50	940	15	298.11	468	84	50	940	15	298.11
			3	0.75	0.1	7193.8	6807	3660	300	168	50	940	15	298.11	384	126	50	940	15	298.11
			3	1	0.1	7193.8	6807	3660	300	168	50	940	15	298.11	300	168	50	940	15	298.11
			3	0.25	0.15	7193.8	6807	3660	300	168	50	940	15	298.11	552	42	50	940	15	298.11
			3	0.5	0.15	7193.8	6807	3660	300	168	50	940	15	298.11	468	84	50	940	15	298.11
			3	0.75	0.15	7193.8	6807	3660	300	168	50	940	15	298.11	384	126	50	940	15	298.11
			3	1	0.15	7193.8	6807	3660	300	168	50	940	15	298.11	300	168	50	940	15	298.11
			3	0.25	0.2	7193.8	6807	3660	300	168	50	940	15	298.11	552	42	50	940	15	298.11
			3	0.5	0.2	7193.8	6807	3660	300	168	50	940	15	298.11	468	84	50	940	15	298.11
			3	0.75	0.2	7193.8	6807	3660	300	168	50	940	15	298.11	384	126	50	940	15	298.11
			3	1	0.2	7193.8	6807	3660	300	168	50	940	15	298.11	300	168	50	940	15	298.11
			3	0.25	0.25	7193.8	6807	3660	300	168	50	940	15	298.11	552	42	50	940	15	298.11
			3	0.5	0.25	7193.8	6807	3660	300	168	50	940	15	298.11	468	84	50	940	15	298.11
			3	0.75	0.25	7193.8	6807	3660	300	168	50	940	15	298.11	384	126	50	940	15	298.11
			3	1	0.25	7193.8	6807	3660	300	168	50	940	15	298.11	300	168	50	940	15	298.11

Table 4: SAC 5 parameters and dimensions (continued)

	Beam	Column	Unitless Parameters			L (mm)	L_b (mm)	L_c (mm)	First pair of voids dimensions						Second pair of voids dimensions					
			α	β	γ				a (mm)	b (mm)	D_v (mm)	L_v (mm)	r_v (mm)	Sc (mm)	a (mm)	b (mm)	Dv (mm)	Lv (mm)	rv (mm)	Sc (mm)
Multi Logitudinal Voids SAC5	W 30*99	W 14*176	4	0.25	0.1	7193.8	6807	3660	300	178	40	940	10	293.11	567	44.5	40	940	10	293.11
			4	0.5	0.1	7193.8	6807	3660	300	178	40	940	10	293.11	478	89	40	940	10	293.11
			4	0.75	0.1	7193.8	6807	3660	300	178	40	940	10	293.11	389	133.5	40	940	10	293.11
			4	1	0.1	7193.8	6807	3660	300	178	40	940	10	293.11	300	178	40	940	10	293.11
			4	0.25	0.15	7193.8	6807	3660	300	178	40	940	10	293.11	567	44.5	40	940	10	293.11
			4	0.5	0.15	7193.8	6807	3660	300	178	40	940	10	293.11	478	89	40	940	10	293.11
			4	0.75	0.15	7193.8	6807	3660	300	178	40	940	10	293.11	389	133.5	40	940	10	293.11
			4	1	0.15	7193.8	6807	3660	300	178	40	940	10	293.11	300	178	40	940	10	293.11
			4	0.25	0.2	7193.8	6807	3660	300	178	40	940	10	293.11	567	44.5	40	940	10	293.11
			4	0.5	0.2	7193.8	6807	3660	300	178	40	940	10	293.11	478	89	40	940	10	293.11
			4	0.75	0.2	7193.8	6807	3660	300	178	40	940	10	293.11	389	133.5	40	940	10	293.11
			4	1	0.2	7193.8	6807	3660	300	178	40	940	10	293.11	300	178	40	940	10	293.11
			4	0.25	0.25	7193.8	6807	3660	300	178	40	940	10	293.11	567	44.5	40	940	10	293.11
			4	0.5	0.25	7193.8	6807	3660	300	178	40	940	10	293.11	478	89	40	940	10	293.11
			4	0.75	0.25	7193.8	6807	3660	300	178	40	940	10	293.11	389	133.5	40	940	10	293.11
			4	1	0.25	7193.8	6807	3660	300	178	40	940	10	293.11	300	178	40	940	10	293.11

Table 5: SAC 3 parameters and dimensions

	Beam	Column	Unitless Parameters			L (mm)	L_b (mm)	L_c (mm)	First pair of voids dimensions						Second pair of voids dimensions					
			α	β	γ				a (mm)	b (mm)	D_v (mm)	L_v (mm)	r_v (mm)	Sc (mm)	a (mm)	b (mm)	Dv (mm)	Lv (mm)	rv (mm)	Sc (mm)
Single Void SAC3	W 24*68	W 14*120				7225.8	6858	3660												
				4		7225.8	6858	3660	210	154	35	755	10	235.24						
				3		7225.8	6858	3660	210	144	45	755	15	240.24						
				2.5		7225.8	6858	3660	210	139	50	755	15	240.24						
				2		7225.8	6858	3660	210	129	60	755	20	245.24						
				1.5		7225.8	6858	3660	210	114	75	755	25	250.24						
				1		7225.8	6858	3660	210	99	90	755	35	260.24						
				0.75		7225.8	6858	3660	210	84	105	755	40	265.24						
				0.5		7225.8	6858	3660	210	69	120	755	50	275.24						
				0.25		7225.8	6858	3660	210	44	145	755	60	285.24						

Table 5: SAC 3 parameters and dimensions (continued)

	Beam	Column	Unitless Parameters			L (mm)	L_b (mm)	L_c (mm)	First pair of voids dimensions						Second pair of voids dimensions					
			α	β	γ				a (mm)	b (mm)	D_v (mm)	L_v (mm)	r_v (mm)	Sc (mm)	a (mm)	b (mm)	Dv (mm)	Lv (mm)	rv (mm)	Sc (mm)
Multi Logitudinal Voids SAC3	W 24*68	W 14*120	2	0.25	0.1	7225.8	6858	3660	210	129	60	755	20	245.24	404	32.25	60	755	20	245.24
			2	0.5	0.1	7225.8	6858	3660	210	129	60	755	20	245.24	340	64.5	60	755	20	245.24
			2	0.75	0.1	7225.8	6858	3660	210	129	60	755	20	245.24	274	96.75	60	755	20	245.24
			2	1	0.1	7225.8	6858	3660	210	129	60	755	20	245.24	210	129	60	755	20	245.24
			2	0.25	0.15	7225.8	6858	3660	210	129	60	755	20	245.24	404	32.25	60	755	20	245.24
			2	0.5	0.15	7225.8	6858	3660	210	129	60	755	20	245.24	340	64.5	60	755	20	245.24
			2	0.75	0.15	7225.8	6858	3660	210	129	60	755	20	245.24	274	96.75	60	755	20	245.24
			2	1	0.15	7225.8	6858	3660	210	129	60	755	20	245.24	210	129	60	755	20	245.24
			2	0.25	0.2	7225.8	6858	3660	210	129	60	755	20	245.24	404	32.25	60	755	20	245.24
			2	0.5	0.2	7225.8	6858	3660	210	129	60	755	20	245.24	340	64.5	60	755	20	245.24
			2	0.75	0.2	7225.8	6858	3660	210	129	60	755	20	245.24	274	96.75	60	755	20	245.24
			2	1	0.2	7225.8	6858	3660	210	129	60	755	20	245.24	210	129	60	755	20	245.24
			2	0.25	0.25	7225.8	6858	3660	210	129	60	755	20	245.24	404	32.25	60	755	20	245.24
			2	0.5	0.25	7225.8	6858	3660	210	129	60	755	20	245.24	340	64.5	60	755	20	245.24
			2	0.75	0.25	7225.8	6858	3660	210	129	60	755	20	245.24	274	96.75	60	755	20	245.24
			2	1	0.25	7225.8	6858	3660	210	129	60	755	20	245.24	210	129	60	755	20	245.24

Table 5: SAC 3 parameters and dimensions (continued)

	Beam	Column	Unitless Parameters			L (mm)	L_b (mm)	L_c (mm)	First pair of voids dimensions						Second pair of voids dimensions					
			α	β	γ				a (mm)	b (mm)	D_v (mm)	L_v (mm)	r_v (mm)	Sc (mm)	a (mm)	b (mm)	Dv (mm)	Lv (mm)	rv (mm)	Sc (mm)
Multi Logitudinal Voids SAC3	W 24*68	W 14*120	3	0.25	0.1	7225.8	6858	3660	210	144	45	755	15	240.24	426	36	45	755	15	240.24
			3	0.5	0.1	7225.8	6858	3660	210	144	45	755	15	240.24	354	72	45	755	15	240.24
			3	0.75	0.1	7225.8	6858	3660	210	144	45	755	15	240.24	282	108	45	755	15	240.24
			3	1	0.1	7225.8	6858	3660	210	144	45	755	15	240.24	210	144	45	755	15	240.24
			3	0.25	0.15	7225.8	6858	3660	210	144	45	755	15	240.24	426	36	45	755	15	240.24
			3	0.5	0.15	7225.8	6858	3660	210	144	45	755	15	240.24	354	72	45	755	15	240.24
			3	0.75	0.15	7225.8	6858	3660	210	144	45	755	15	240.24	282	108	45	755	15	240.24
			3	1	0.15	7225.8	6858	3660	210	144	45	755	15	240.24	210	144	45	755	15	240.24
			3	0.25	0.2	7225.8	6858	3660	210	144	45	755	15	240.24	426	36	45	755	15	240.24
			3	0.5	0.2	7225.8	6858	3660	210	144	45	755	15	240.24	354	72	45	755	15	240.24
			3	0.75	0.2	7225.8	6858	3660	210	144	45	755	15	240.24	282	108	45	755	15	240.24
			3	1	0.2	7225.8	6858	3660	210	144	45	755	15	240.24	210	144	45	755	15	240.24
			3	0.25	0.25	7225.8	6858	3660	210	144	45	755	15	240.24	426	36	45	755	15	240.24
			3	0.5	0.25	7225.8	6858	3660	210	144	45	755	15	240.24	354	72	45	755	15	240.24
			3	0.75	0.25	7225.8	6858	3660	210	144	45	755	15	240.24	282	108	45	755	15	240.24
			3	1	0.25	7225.8	6858	3660	210	144	45	755	15	240.24	210	144	45	755	15	240.24

Table 5: SAC 3 parameters and dimensions (continued)

	Beam	Column	Unitless Parameters			L (mm)	L_b (mm)	L_c (mm)	First pair of voids dimensions						Second pair of voids dimensions					
			α	β	γ				a (mm)	b (mm)	D_v (mm)	L_v (mm)	r_v (mm)	Sc (mm)	a (mm)	b (mm)	Dv (mm)	Lv (mm)	rv (mm)	Sc (mm)
Multi Logitudinal Voids SAC3	W 24*68	W 14*120	4	0.25	0.1	7225.8	6858	3660	210	154	35	755	10	235.24	441	38.5	35	755	10	235.24
			4	0.5	0.1	7225.8	6858	3660	210	154	35	755	10	235.24	364	77	35	755	10	235.24
			4	0.75	0.1	7225.8	6858	3660	210	154	35	755	10	235.24	287	115.5	35	755	10	235.24
			4	1	0.1	7225.8	6858	3660	210	154	35	755	10	235.24	210	154	35	755	10	235.24
			4	0.25	0.15	7225.8	6858	3660	210	154	35	755	10	235.24	441	38.5	35	755	10	235.24
			4	0.5	0.15	7225.8	6858	3660	210	154	35	755	10	235.24	364	77	35	755	10	235.24
			4	0.75	0.15	7225.8	6858	3660	210	154	35	755	10	235.24	287	115.5	35	755	10	235.24
			4	1	0.15	7225.8	6858	3660	210	154	35	755	10	235.24	210	154	35	755	10	235.24
			4	0.25	0.2	7225.8	6858	3660	210	154	35	755	10	235.24	441	38.5	35	755	10	235.24
			4	0.5	0.2	7225.8	6858	3660	210	154	35	755	10	235.24	364	77	35	755	10	235.24
			4	0.75	0.2	7225.8	6858	3660	210	154	35	755	10	235.24	287	115.5	35	755	10	235.24
			4	1	0.2	7225.8	6858	3660	210	154	35	755	10	235.24	210	154	35	755	10	235.24
			4	0.25	0.25	7225.8	6858	3660	210	154	35	755	10	235.24	441	38.5	35	755	10	235.24
			4	0.5	0.25	7225.8	6858	3660	210	154	35	755	10	235.24	364	77	35	755	10	235.24
			4	0.75	0.25	7225.8	6858	3660	210	154	35	755	10	235.24	287	115.5	35	755	10	235.24
			4	1	0.25	7225.8	6858	3660	210	154	35	755	10	235.24	210	154	35	755	10	235.24

3.2 The Proposed Beam End Configuration (BEC)

3.2.1 Details of the BEC

Details of the proposed BEC are shown in Figure 38. Effective parameters in the geometry of the proposed BEC are listed below:

D_{v1}: Depth of the first pair of voids

D_{v2}: Depth of the second pair of voids

L_V: Length of each void

a_1: Perpendicular clear distance between the first pair of voids

a_2: Perpendicular clear distance between the second pair of voids

D: Beam overall depth and also the horizontal distance from the face of the column to the center of the first pair of voids.

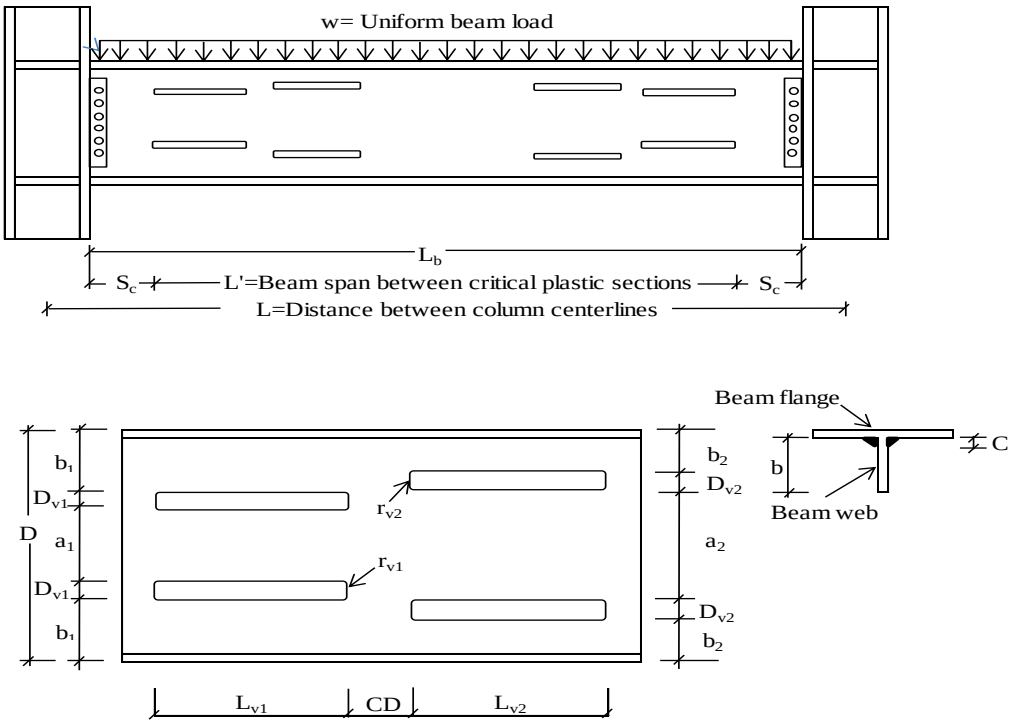

Figure 38: Details of the proposed BEC in multi longitudinal voids

The equation for minimum required shear depth (Equation 1) (ANSI/AISC 360-10, 2010) can be used to determine the minimum clear vertical distance, parameters a_1 and a_2, between the two voids.

$$\phi R_n = 0.9 \times 0.6 \times f_y \times A_g \quad (1)$$

where,

ϕR_n is total shear force at beam cross section and can be obtained from $M_p/(L_b/2)$

f_y is the nominal yield strength of beam

A_g is gross shear area ($A_g = a \times t_w$, t_w is the beam web thickness).

If the over strength factor is taken as 1.2 AISC-LRFD (1995) then Equation 1 can be simplified to find the minimum required shear depth, a_1 and a_2, as follows:

$$a_1 = \frac{5.29 \times Z_b}{L_b \times t_w} \quad (2)$$

where, Z_b is the plastic section modulus of the beam.

Parameter a_1 is equal to 465 mm (SAC7), 300 mm (SAC5) and 210 mm (SAC3). The horizontal length of each void is 1.25 times the beam overall depth ($L_{V1}=L_{V2}=1.25D$). The minimum value of parameter *b* (see Figure 3) is 1.4 times the parameter *c*, where *c* is the root radius of the beam (*b*=1.4*c*). The factors 1.25 and 1.4 were selected based on the parameteric study done by Hedayat and Celikag (2009) for RBW connections with single longitudinal voids. The first pair of voids was located as such that their distance from center of voids to the face of column was equal to the overall depth of the beam (Figure 38). Void depth D_{v1} was achieved by

Equation 3, where t_f is the beam flange thickness and b_1 is as shown as on the inset figure in Figure 4. In this study, for all cases, the same size of voids were used ($D_{V1}=D_{V2}$).

$$D_{v1} = [(D-2t_f-a_1)/[2((b_1/D_{v1})+1)]] \quad (3)$$

The radii of the corners of rectangular voids (parameter r_v) was obtained from ASCE standard, SEI/ASCE23-97 (1997) and Equation 4. It was mentioned in reference ANSI/AISC 360-10 (2010) that $r_v \geq 2t_w$, where smallest t_w is 8 mm. However, in the same reference, r_v=9.5 mm was permitted. On the other hand, to use small r_v, smoother surface should be provide by drilling ASCE standard. SEI/ASCE23-97 (1997).

$$r_v \text{ (mm)} = (D_V\text{-}20\text{mm})/2 \quad (4)$$

Other design parameters are defined in the following section.

3.2.2 Design parameters

The three selected SAC specimens 3, 5 and 7 were used for the parametric investigation which was carried out on the geometry of the voids by defining three design parameters, α, β and γ. These parameters are defined as follows:

Parameter α: This parameter is the ratio of b_1 to D_{v1} ($\alpha= b_1/D_{v1}$ where b_1 and D_{v1} are as shown in Figure 38). The values used for parameter α were 2, 3 and 4. Hence, by assuming the value of this parameter the first pair of voids depth (parameter D_{V1}) can be obtained by using Equation 3.

Parameter β: This parameter is the ratio of b_2 to b_1 which are shown in Fig.4 ($\beta=b_2/b_1$). Four different values were used for parameter β; 1, 0.75, 0.5 and 0.25.

Hence, by assuming the value of this parameter and knowing D_{V2} ($D_{V2}=D_{V1}$), the perpendicular distance of the second pair of voids (parameter a_2) can be obtained. However, this value cannot be less than the value obtained from Equation 2. It should be noted that, in this study, the value of parameter a_1 was directly obtained from Equation 2.

Parameter γ: This parameter is the ratio of the horizontal clear distance between the first and the second voids to the void length ($\gamma=CD/L_v$). The values used for parameter γ were 0.1, 0.15, 0.2 and 0.25.

Chapter 4

ANALYTICAL RESULTS AND DISCUSSIONS

4.1 Typical Behavior of the modified Post-Northridge Connection

Hedayat and Celikag (2009) attempted to improve the post-Northridge connections ductility and strength by using one pair of longitudinal voids at the beam web (Figure 4). This modification was effective to limit the stress concentrations at the complete joint penetration (CJP) groove welds at the column face and to provide more energy dissipation along the beam length. Note that this method was effective for beams with the overall depth less than 750 mm. However, for deeper beams, where the depths of voids were large, this method alone was not adequate. Hence, for deep beams, in order to delay or prevent the beam web buckling and increase the connection ductility, they proposed the use of tubes and web stiffeners at the beam web area (Figure 4).

Figure 39 shows the PEEQ distribution for modified specimen SAC7 with deep beam W36x150 (beam overall depth = 912 mm) in the case of using a single pair of voids at four percent total rotation (sub step=52 in ANSYS program). This figure clearly shows the PEEQ concentrations at the RBW area and excessive lateral torsional buckling of the beam web which was due to the use of large voids at the beam web area. These finally led to fracture at the void area before the total rotation reached four percent.

The PEEQ distribution of the same specimen with multi longitudinal voids at five percent total rotation (sub step=65 in ANSYS program) are given in Figure 40. Note that, in this case, due to the use of multi voids, the depths of voids became smaller when compared to the ones used in Figure 39. According to this figure, PEEQ strains are more uniformly distributed between multi voids, such that the normalized PEEQ (plastic equivalent strain divided by yield strain) at the most critical location of a connection (i.e. at the root of weld access hole) reduced from 92.77 for the beam with single pair of voids to 46.01 for multi-void specimen. In addition, multi voids caused considerable reduction in the PEEQ concentration at the beam flange at the start level of the first pair of voids (see Figure 40). It caused a remarkable delay in the connection failure time such that the total rotation at the column web center of this specimen could easily exceed 5 percent. The moment-rotation curve of this specimen is shown in Figure 41 where a remarkable delay is apparent in the onset of the beam web local buckling when compared to the same specimen with single voids. Figure 41 shows that the initial rotational stiffness of the two specimens are approximately the same. However, multi longitudinal voids specimens undergone earlier yielding in the yielding region, but they achieved much more ductility and strength when compared to the single pair of voids.

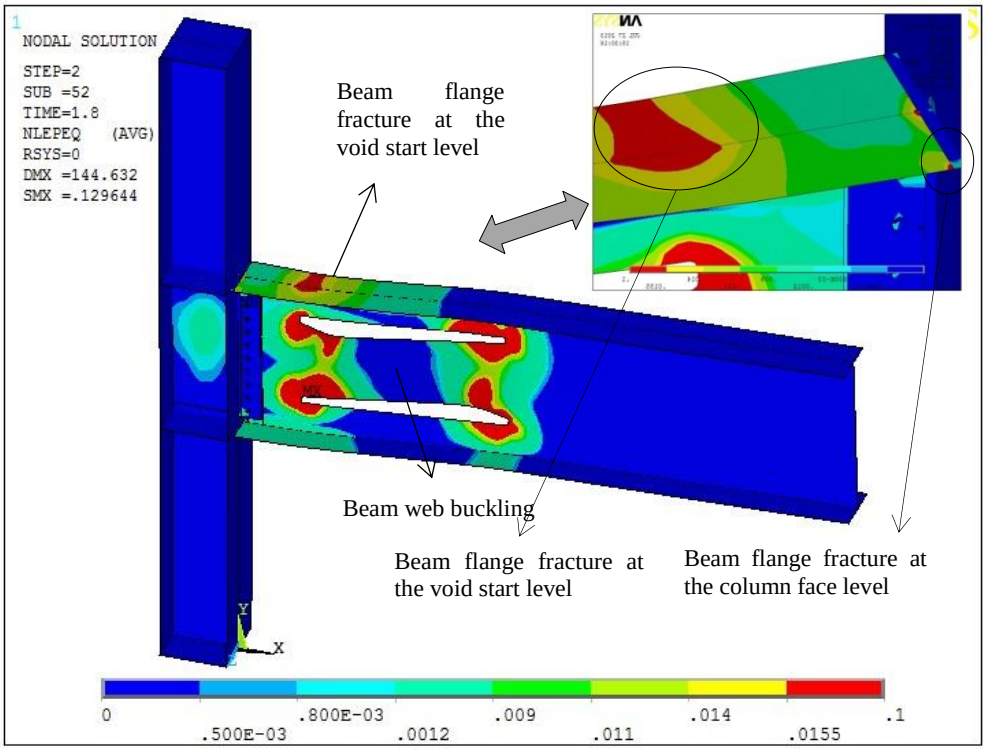

Figure 39: PEEQ distribution for modified specimen SAC7 with single voids at four percent total rotation

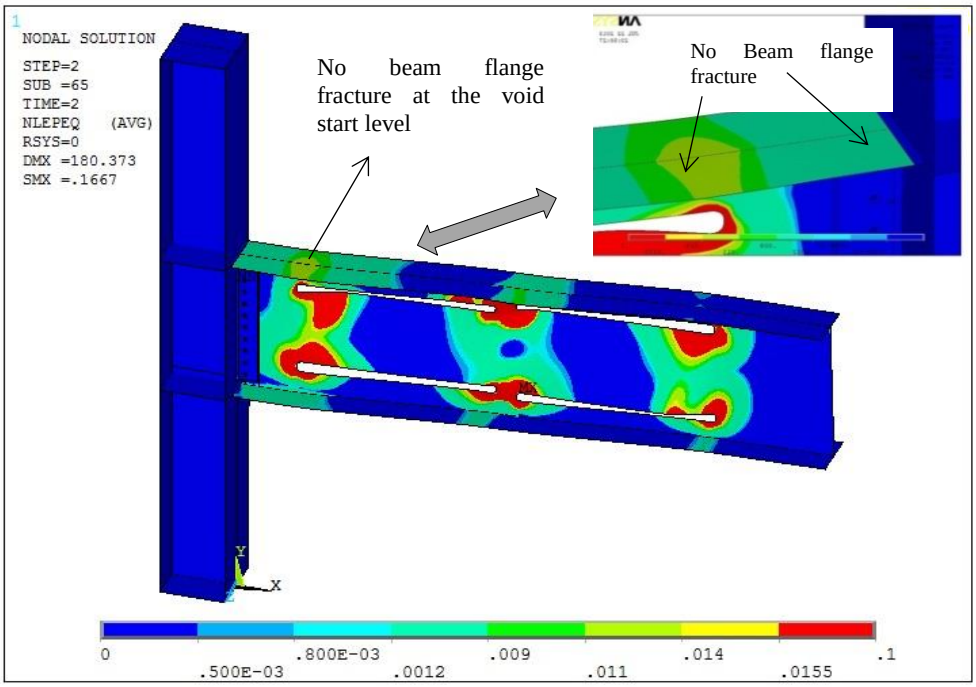

Figure 40: PEEQ distribution for modified specimen SAC7 with multi voids at five percent total rotation

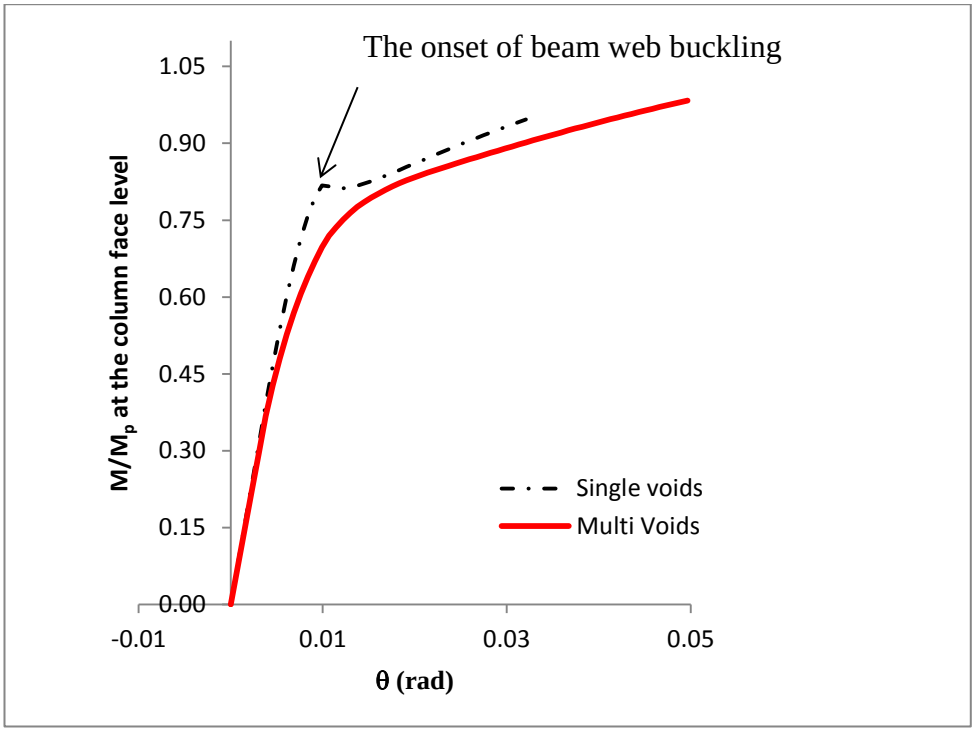

Figure 41: Normalize moment-rotation curves of modified specimens SAC7 with single and multi-longitudinal voids

4.2. Effect of Design Parameters on the Strength and Ductility of the Modified Post-Northridge Connections

Figures 42 through 44 show the effect of design parameters α, β and γ on the ductility of the modified specimens SAC7, SAC5 and SAC3. Connection ductility was evaluated by using parameter θ_{CWC}, which is the total rotation of the connection at the center of column web. It is calculated by dividing the beam tip deflection by a distance measured from the beam tip to the center of the column web.

By increasing parameter α, the depth of the first pair of voids (i.e. parameter D_{V1}) decreases and the depth of the T-sections (parameter b_1) at the top and bottom of the rectangular voids increases. For most of the specimens (except for few modified specimens of SAC7) as this parameter increased, the connection ductility decreased which can be due to the reduction in the energy dissipation capacity of the beam at

the first pair of voids area (Figures 42 to 44). Results indicate that the highest connection ductility was achieved when parameter α was equal to 2. It should be noted that the initial investigations showed that smaller value may not be desirable since it caused a remarkable reduction in the lateral-torsional/flexural stiffness of the T-sections at the top and bottom of the rectangular voids. It consequently promoted the onset of the torsional buckling of the beam web and flexural buckling of the T-sections.

Initial investigations of the behavior of the proposed BEC showed that the second pair of voids must be located at a closer vertical distance to the beam flange surface when compared to the first pair of voids. This significantly helped to increase the efficiency of the second pair of voids to decrease the strain concentration at the region of the first pair of voids and consequently to uniformly distribute the plastic equivalent strains along the beam length. For this reason, the value of parameter β (β=b_2/b_1) varied between 1 and 0.25. By decreasing parameter β the value of parameter b_2 decreased. Since the first and the second pair of voids have same depth ($D_{V1}=D_{V2}$), it caused an increase in parameter a_2 and consequently moved the second pair of voids up. As it is clear from the Figures 42 to 44, the excessive decrease in parameter β was not desirable. Since it caused a remarkable increase in the PEEQ at the beam flange at the second voids area and promoted the beam flange fracture at this area and finally caused a significant reduction in the connection ductility. The highest connection ductility was achieved for β equal to 1 or 0.75.

By decreasing parameter γ, the horizontal distance between the voids reduces. This helped to increase the efficiency of the second pair of voids and reduced the strain concentrations at the column face region and at the area of the first pair of voids.

However, excessive decrease in this parameter was also detrimental (i.e. γ less than 0.1) since it caused excessive beam web buckling in the area between the first and the second pair of voids and consequently reduced connection strength and ductility. Initial investigations indicated undesirable behavior of connection in the case of using parameter γ less than 0.1. It should be noted that higher values of parameter γ was also undesirable since it significantly reduced the efficiency of the second pair of voids by uniformly distributing the plastic equivalent strains along the beam length and it caused an excessive increase in the strain concentration at the column face region and at the area of the first pair of voids. Based on this discussion, parameter γ varied between 0.1 and 0.25. Considering the finite element results in Figures 42 to 44 and the ductility of connection, it might be concluded that 0.1 is the optimum value for parameter γ.

Figures 45 to 47 show the effect of design parameters α, β and γ on the strength of the modified specimens SAC7, SAC5 and SAC3. Connection strength was evaluated by using the M/M_P ratio which is the ratio of the applied moment measured at the column face level at the failure time to the full beam plastic moment capacity at the column face level. This comparison was done for monotonic loading.

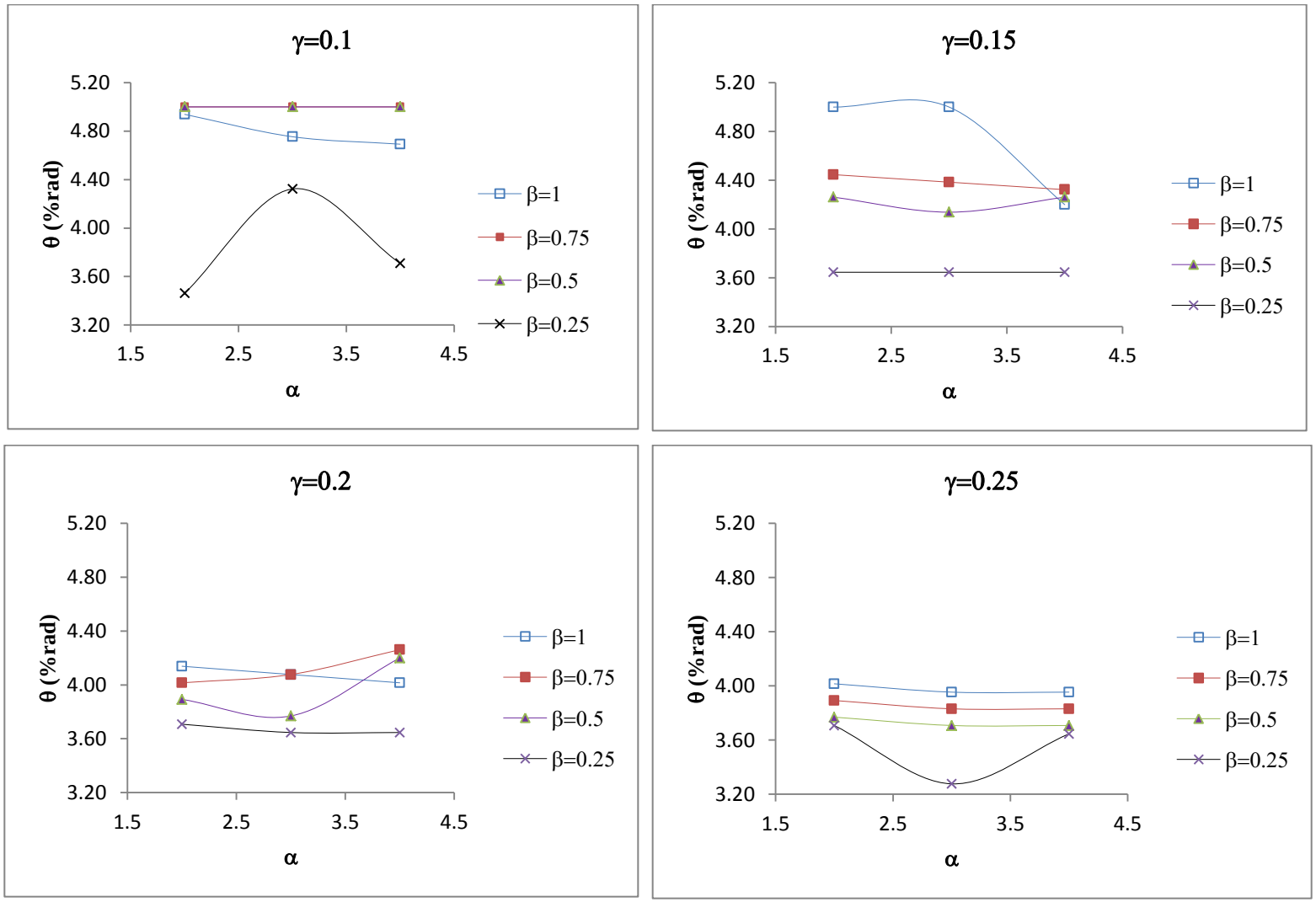

Figure 42: θ versus α for different values of β and γ for SAC7

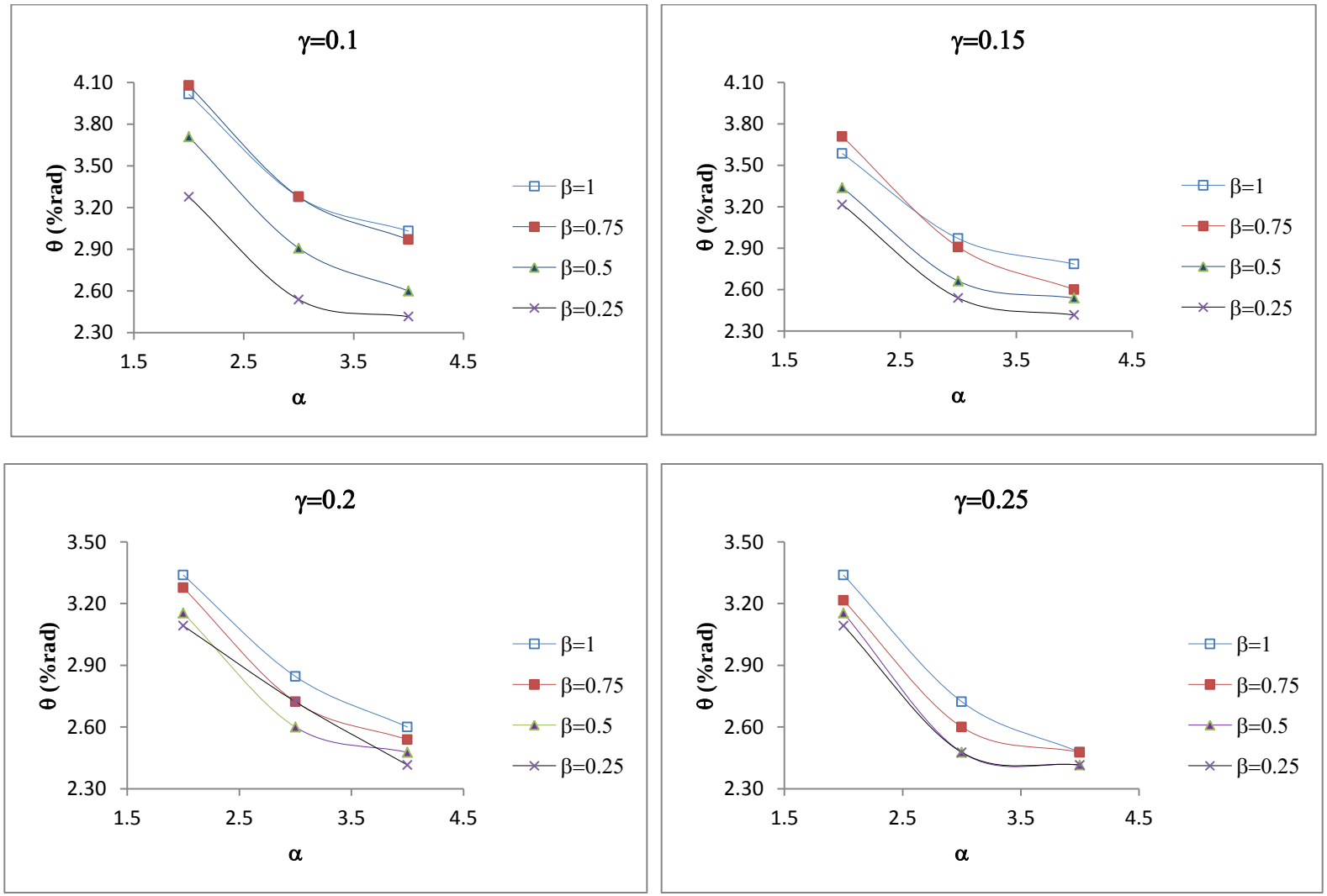

Figure 43: θ versus α for different values of β and γ for SAC5

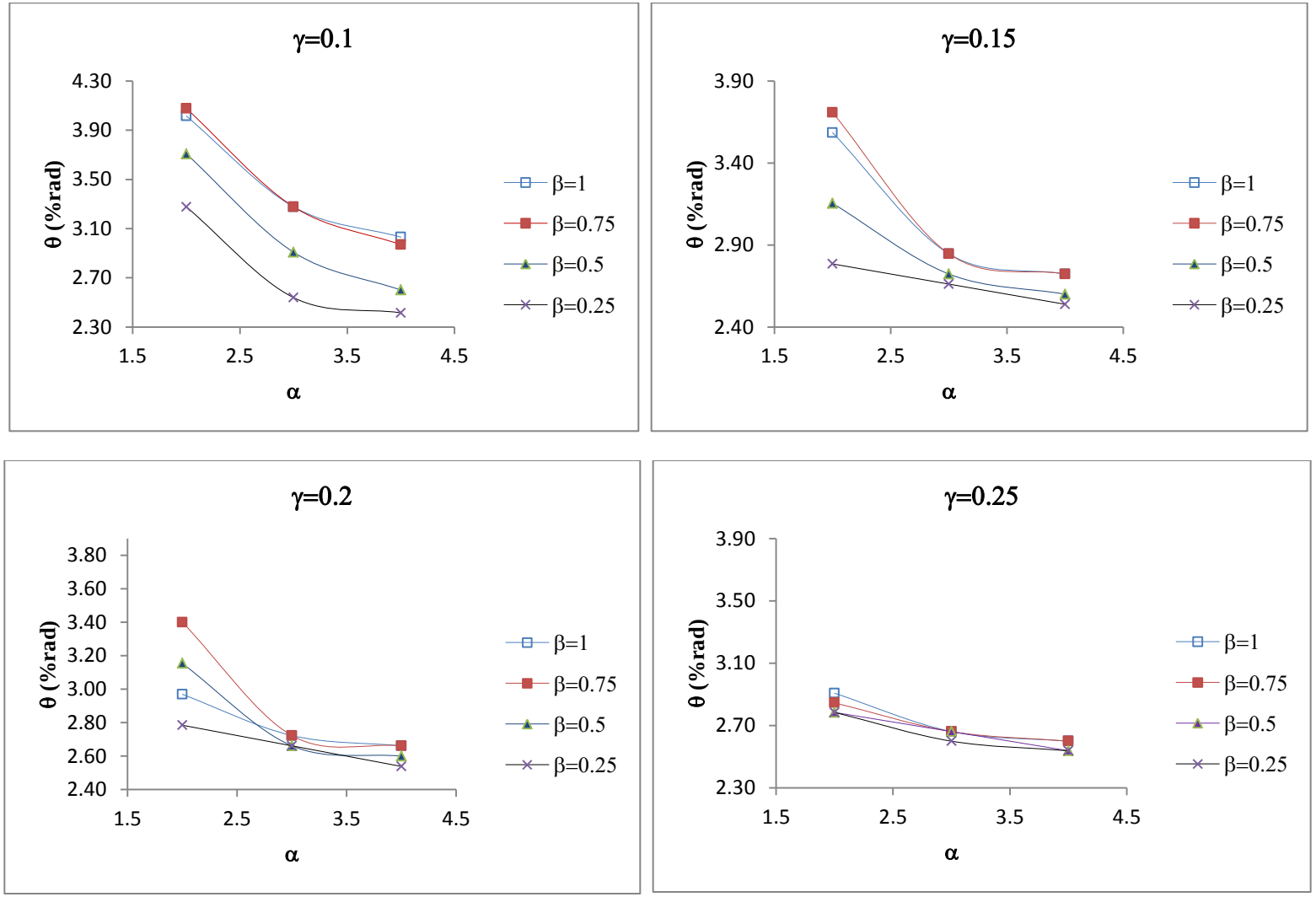

Figure 44: θ versus α for different values of β and γ for SAC3

For most of the modified specimens (parameter β equal to 1, 0.75 and 0.5 and any value of parameter γ) increase in parameter α caused a gradual increase in the connection strength. This was due to the decrease in the depth of the first pair of voids and consequently increase in the depth of the T-sections (parameter b_1) remained at the top and bottom of the first rectangular voids which finally resulted in the enhancement of the flexural and torsional stiffness of the T-sections. For specimens of β equal to 0.25, increase in parameter α caused a significant increase in the connection strength. It should be noted that for these specimens the second pair of horizontal voids was located at the nearest distance from the top surface of the beam flange. In other words, in these specimens the T-sections remained at the top and the bottom of the second pair of rectangular voids had the smallest depth and largest slenderness ratio. As a result, for these specimens increase in parameter α, indirectly decreased the slenderness ratio of the second T-sections and caused the highest increase in the connection strength. However, specimens with β equal to 0.25 had the smallest ductility when compare to the other specimens.

As it is clear from the Figures 45 to 47, decrease in parameter β (from 1 to 0.5) had very small effect on the connection strength degradation. For most of these specimens, the value of M/M_P ratio was greater than 1.05. However, excessive decrease in this parameter (i.e. β=0.25) caused a remarkable reduction in the connection strength which was due to the excessive increase in the slenderness ratio of the T-sections remained at the top and the bottom of the second pair of the rectangular voids. On the other hand by increasing parameter γ and consequently increasing the clear distance between the voids the connection strength slightly increased. However, as mentioned above it caused a reduction in the connection strength.

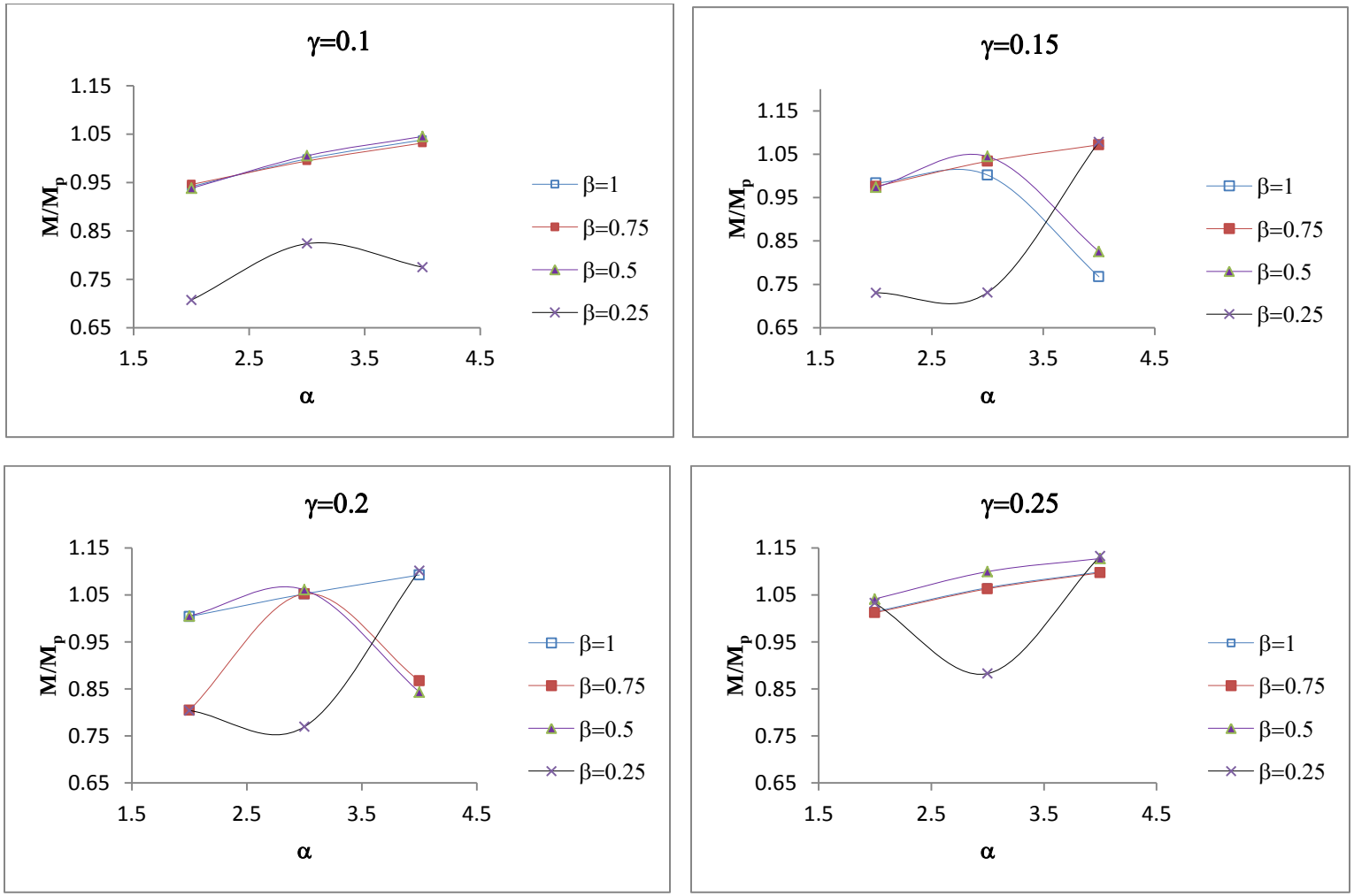

Figure 45: M/M_P versus α for different values of β and γ for SAC7

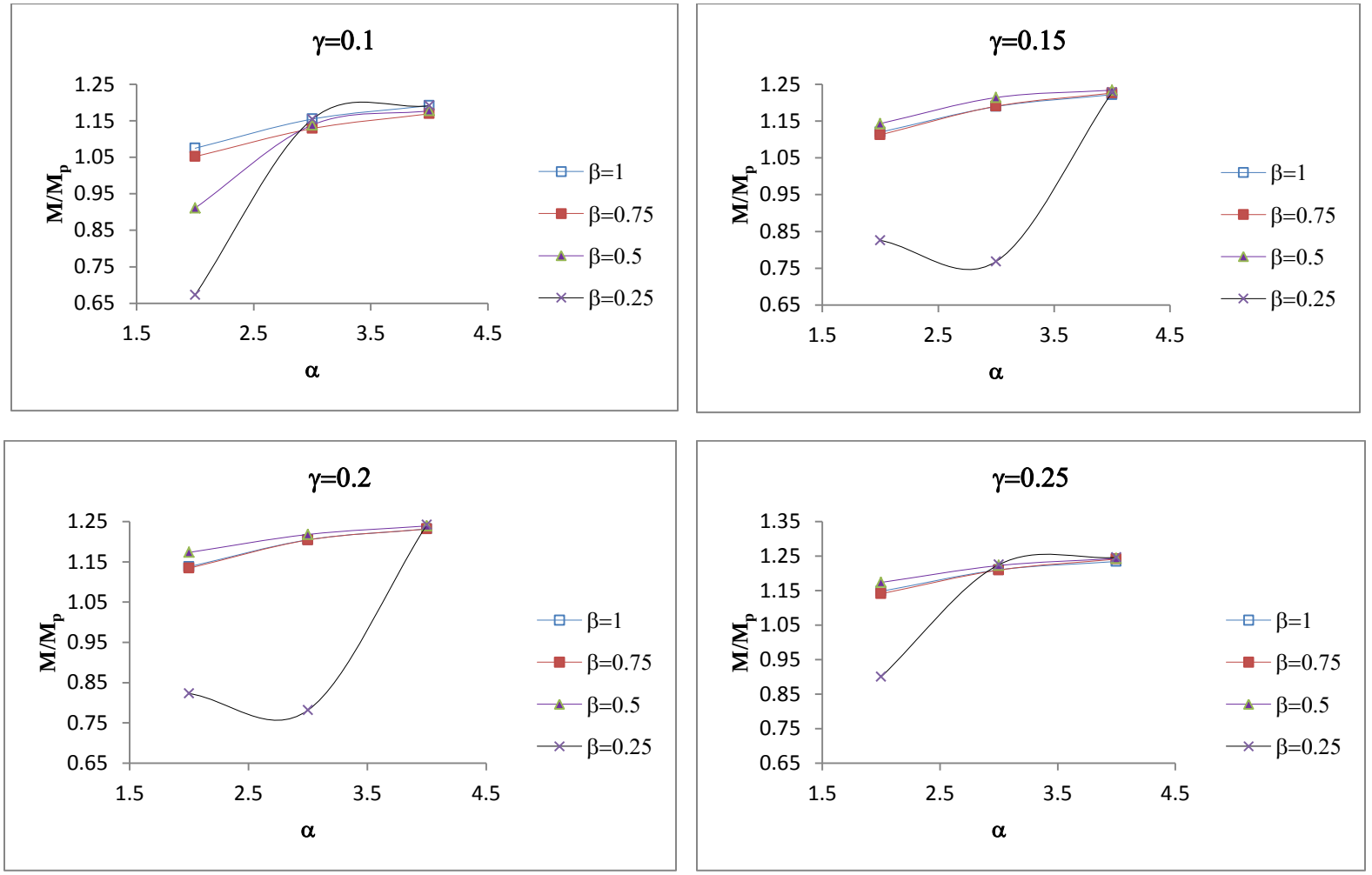

Figure 46: M/M_P versus α for different values of β and γ for SAC5

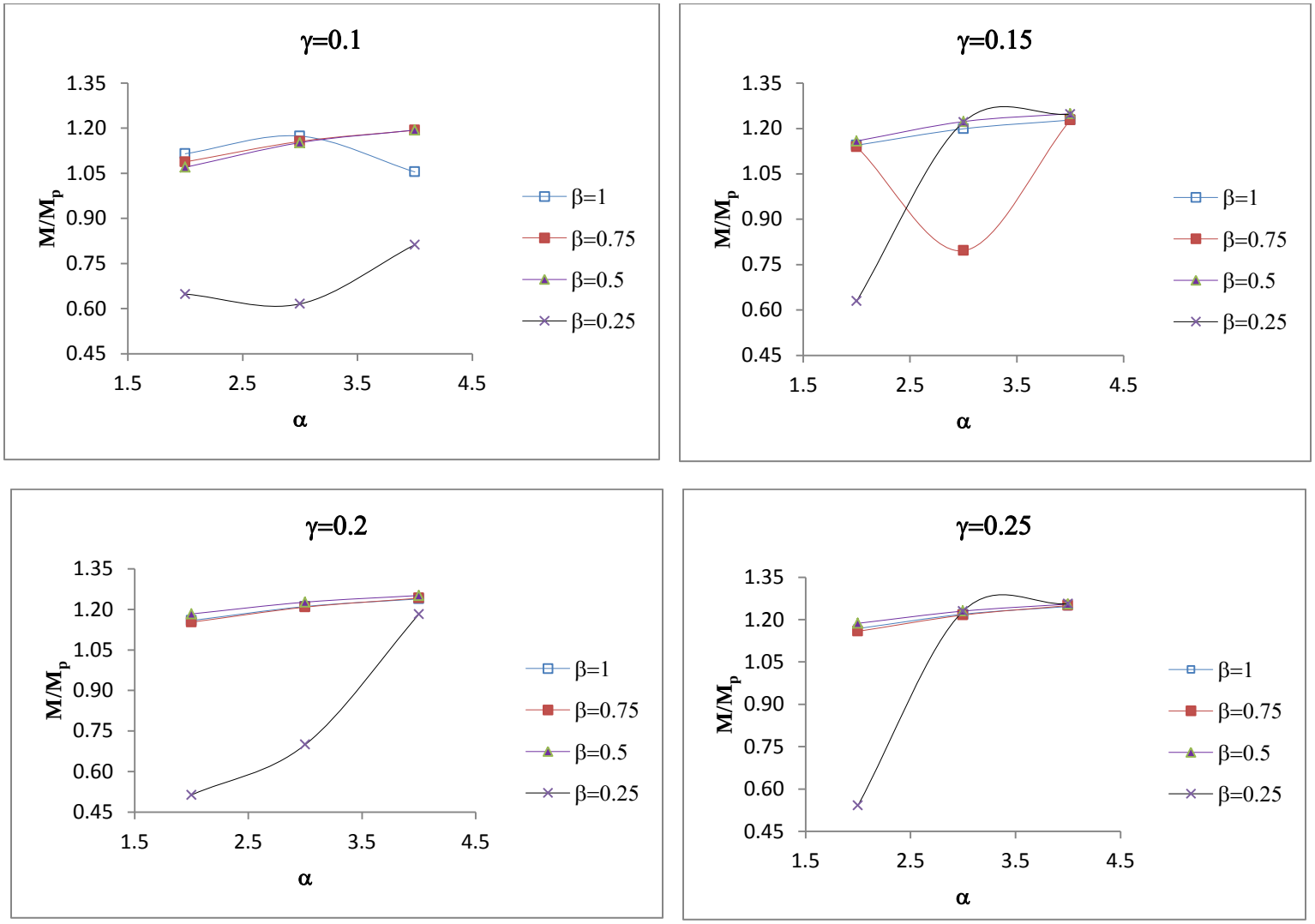

Figure 47: M/M_P versus α for different values of β and γ for SAC3

4.3 Cyclic loading effects

Under cyclic loading, connection strength is generally lower than the one obtained under monotonic loading. It is due to the beam flange and web local buckling. In this study all specimens with adequate strength and ductility (i.e. those specimens of the optimum values of parameters α, β and γ) were re-analyzed under cyclic loading to determine the amount of strength degradation. Thus, the suggested time hysteresis by FEMA350 (2000) is selected as shown in Figure 48. For instance, in Figures 49 and 50 the moment-rotation curves of SAC7 and SAC3 for α, β and γ equal to 2, 0.75 and 0.1 respectively are compared for both monotonic and cyclic loading. It can be seen from the figures that there was no remarkable difference between the connection strength obtained from the two loading types. There was only a small amount of reduction in the connection strength which was due to the local buckling at the RBW area. For both modified specimens SAC7 and SAC3, the connection strength is greater than the minimum required strength, $M/M_P=0.8$.

Figure 49 also shows a pinching in the hysteresis curve of specimen SAC7 which was due to the beam flange/web buckling at the RBW area. By decreasing the beam overall depth, for shallower beam specimen SAC3, the amount of pinching significantly reduced (Figure 50). The hysteresis curve was more stable with an insignificant amount of pinching and this was also due to increase in the parameters α, β and γ.

Similar behavior was also observed for modified specimen SAC5. Hence, it might be concluded that the modified SAC specimens have adequate strength to be used in seismic regions. According to the results of the investigation of connections subject

to both monotonic and cyclic loading (Ricles et al. (2003) and El-Tawil et al. (1998)), it is clear that the monotonic loading could be used to represent cyclic loading conditions.

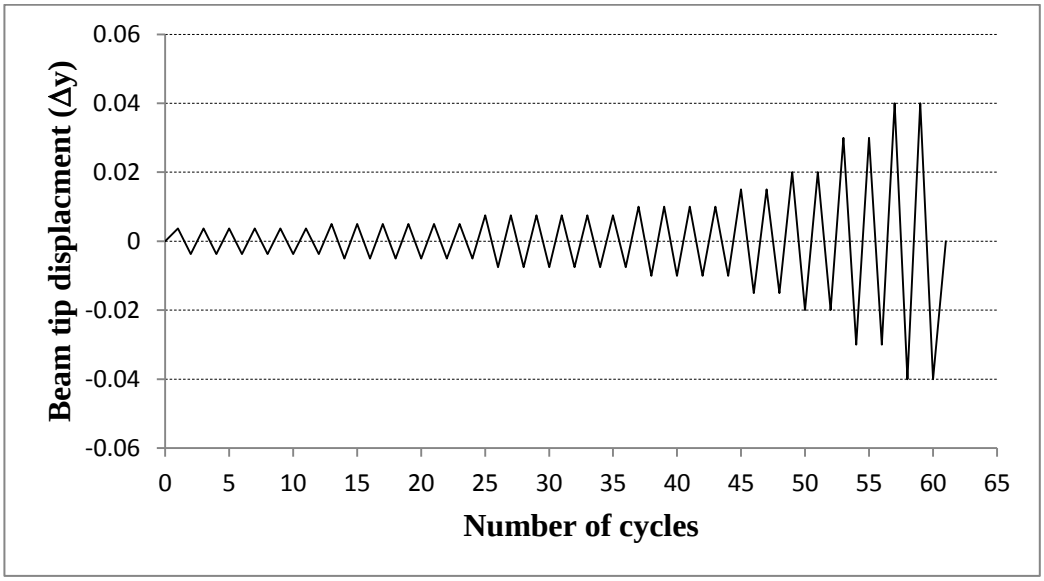

Figure 48: The load history used by FEMA350. (2000)

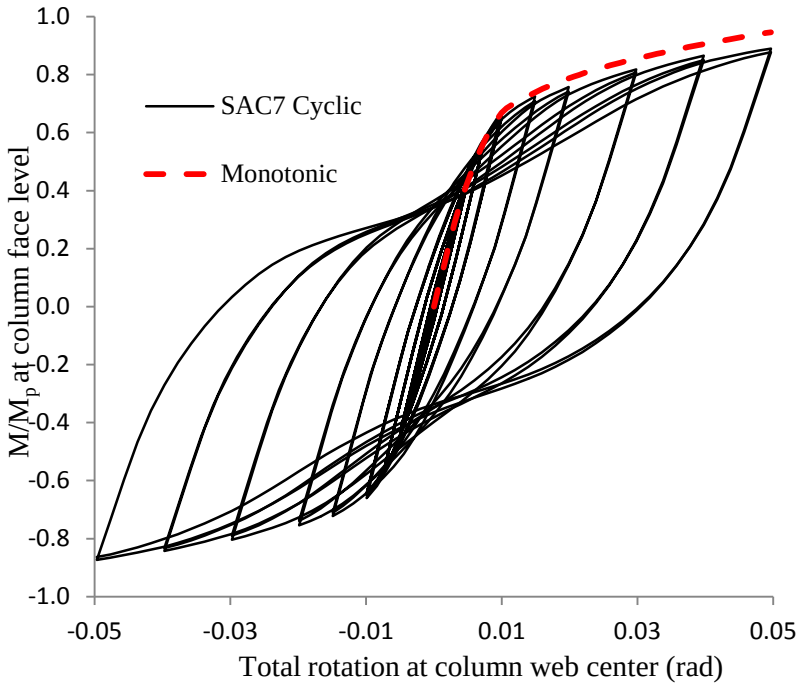

Figure 49: Normalized moment rotation curve of specimen SAC7 for α=2, β=0.75 and γ=0.1

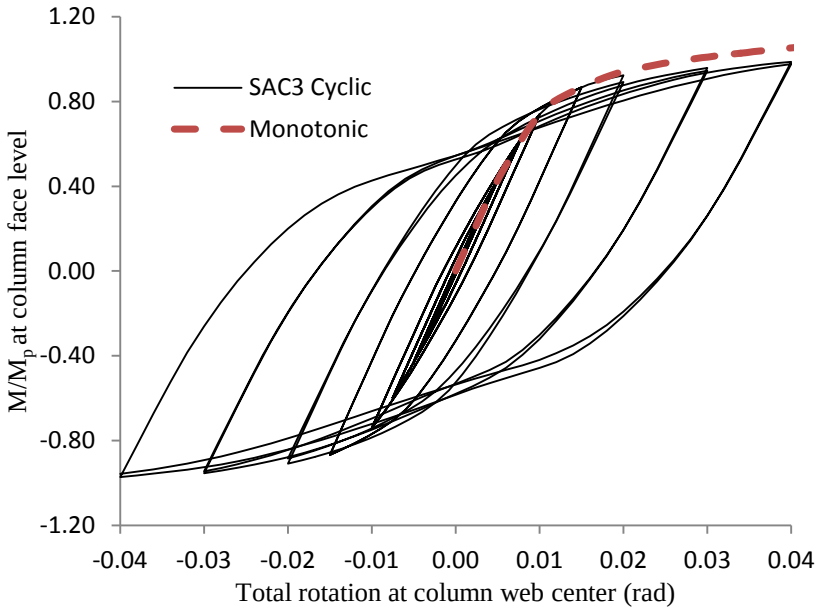

Figure 50: Normalized moment rotation curve of specimen SAC3 for α=2, β=0.75 and γ=0.1

4.4 Summary of results

According to ANSI/AISC 341-10 (2010), the following requirements should be satisfied for the design of beam-to-column connections in buildings constructed in areas with seismic hazard.

1. A story drift angle of at least 0.04 radian should be accommodated by the connections.

2. At a story drift angle of 0.04 radian, the connection flexural resistance at the column face should be equal to at least $0.80M_P$ of the connected beam.

Based on the discussion presented in the previous section and with respect to the requirements mentioned in the above paragraph, from the strength and ductility point of views, for all modified SAC specimens, the highest connection performance might be achieved for α=2, β=0.75 and γ=0.1. The specimens under consideration for this

study easily achieved the minimum required strength. The maximum ductility achieved for these specimens were 5.0, 4.08 and 4.08 percent radian for beam depths of 912 mm, 750 mm and 600 mm respectively which are all greater than the minimum required ductility of 4 percent radian and considerably higher than the results of the SAC group for the same connections, around 2 to 3 percent radian.

Despite of the improvement in the ductility of SAC5 and SAC3, the results indicate that the proposed BEC would be more effective for deep beams rather than shallow beams. The reason can be as follows: The usage of the longitudinal voids is the key parameter for the enhancement of connection ductility for the BECs presented in reference (Hedayat and Celikag, 2009) and in this study. In this study the length of voids was considered as 1.25 times the beam overall depth. Hence, for deeper beams the voids were longer and dissipate more seismic energy when compared to the shallower beams where the voids are shorter. This might be the reason for deeper beams achieving higher ductility than the shallower beams of the proposed BEC.

Chapter 5

GENERALIZED DESIGN PROCEDURE

The modification procedure presented in the previous chapter is easy for application. However, the following parameters were neglected; gravity effect, beam length and moment gradient. In this chapter, these parameters are not neglected. Instead they are used to generalize the design procedure so that the proposed modifications can be applied to other sections. FEMA350 (2000) and Engelhardt et al. (2003) had similar generalized design procedure for RBS.

The design method is based on the limiting moment, M_{pd} (Equation 5), and the associated shear force, V_{pd} (Equation 6), at critical plastic section, which is the starting point of the first pair of voids. The critical plastic section is denoted in Fig.3 by parameter S_C and can be obtained by using Equation 7.

$$M_{pd} = C_{pr} \times Z_{RBWS} \times F_{ye} \quad (5)$$

$$V_{pd} = 2M_{pd} / L' + wL'/2 \quad (6)$$

$$S_C = D - L_{V1}/2 + r_V \quad (7)$$

$$Z_{RBWS} = Z_b - D_{V1} \times t_w \times (a_1 + D_{V1}) \quad (8)$$

In these equations F_{ye} is the expected yield stress of material, Z_{RBWS} is plastic section modulus at RBW area (Equation 8), *w* is the factored gravity loads on the beam and parameter L' is shown in Figure 38. The moment at the column face, M_f, is

$$M_f = M_{pd} + V_{pd} \times S_C \tag{9}$$

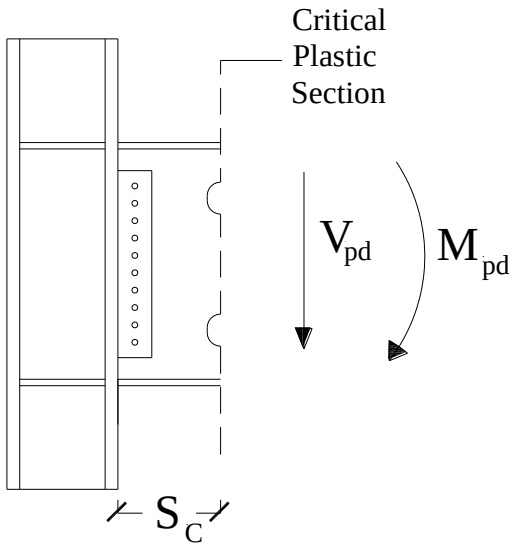

Figure 51: Shear force and bending moment of the critical section

In order to obtain the maximum normalized moment at beam-column weld location, η_t, equations (5) and (6) are substituted into equation (9) and then both sides were normalized with respect to the full section plastic moment of beam ($Z_b.F_{ye}$).

$$\eta_t = \eta_g + \eta_e = \frac{w \times L' \times S_C}{2Z_b \times F_{ye}} + C_{pr} \times \frac{Z_{RBWS}}{Z_b}(1 + \frac{2S_C}{L'}) \tag{10}$$

The effect of gravity and the seismic loads are considered by η_g, and η_e respectively. For simplicity, the influence of the segment of gravity load was neglected within the length S_C. To enhance the ductility of a post-Northridge connection, the longitudinal voids configuration (parameters α, β and γ), must be chosen as such to keep the value of η_t within a suitable interval to avoid beam flange fracture at RBW and WAH regions prior to achieving 4 percent total rotation.

For any modified connection η_t can be found by using analytical and experimental results. For example, η_t is 1.05 (Engelhard et al., 2003) and 1.15 (FEMA 350, 2000) for RBS connections with bottom flange cut and both top and bottom beam flange cut respectively. However, in the study done by Hedayat and Celikag (2009) for RBW connections with single rectangular voids, depending on the beam overall depth and the connection type, a range of appropriate η_t values (between 1.05 and 1.14) was proposed. The normalized moment, developed at the column face, $\eta_t = M/M_P$, for all modified specimens are graphically shown in Figures 45 to 47. Appropriate values of parameter η_t can be determined by comparing its values (Figures 45 to 47) with the connection ductility, θ_{cwc} (Figures 42 to 44). Despite being difficult to select, based on the data presented in Figures 42 to 44, a value between 0.95 and 1.02 might be the best value of parameter η_t. However, according to the finite element results, a value closer to the lower bound might be more appropriate for deeper beams (beam depth$\geq$750 mm) while a value closer to the upper bound might be more suitable for shallower beams.

C_{pr} in Equation (5) is a factor to account for the maximum connection strength, including strain hardening, local restraint and additional reinforcement. In FEMA350 (2000), the C_{pr} factor is given by equation $(f_y+f_u)/2f_y$, where f_u and f_y are the specified minimum tensile and yield stresses of material respectively. C_{pr} value of 1.2 is generally suggested to be used for modified connections by FEMA350 (2000). This factor is the ratio of the measured moment at the starting point of the first pair of voids (S_c) at the connection failure time to the beam plastic moment capacity at this location. This factor is a function of the configuration and the size of voids for the proposed BEC. In this study, the nonlinear model given in Equation 11 was used to estimate the C_{pr} factor, based on the design parameters α, β, γ and beam flange and

web slenderness ratios. In this equation b_f, t_f and t_w are the beam flange width and thickness and the beam web thickness respectively. Constant C_1 and exponents C_2 to C_6 were determined using regression analyses and are summarized in Table 6. The last column of Table 6 gives the observed average error. This error is the mean square error which emphasizes the effect of large errors ($\sum_{1}^{n}(real\ C_{pr} - estimated\ C_{pr})^2$, n is total number of data).

$$C_{pr} = C_1 \times \alpha^{C2} \times \beta^{C3} \times \gamma^{C4} \times [(D - 2t_f)/t_w]^{C5} \times (b_f / t_f)^{C6} \qquad (11)$$

The connection ductility can also be estimated using Equation 12 once the geometry of proposed BEC is finalized. Constant C_1 and exponents C_2 to C_7 were determined using regression analyses and are summarized in Table 6. The last column of Table 6 gives the average of mean square error observed for all SAC specimens.

$$\theta_{CWC} = C_1 \times \alpha^{C2} \times \beta^{C3} \times \gamma^{C4} \times [(D - 2t_f)/t_w]^{C5} \times (b_f / t_f)^{C6} \times (L_b / D)^{C7} \qquad (12)$$

Note that in order to use equations (11) and (12), all design principles presented in section 4 should be considered (i.e. $L_{V1}=L_{V2}=1.25D$; $D_{V1}=D_{V2}$; $a_1 = 5.29 \times Z_b / (L_b . t_w)$; $a_2 \geq a_1$ and the distance from the center of the first pair of voids to the column face is equal to the beam overall depth, D).

Table 6: Variables C1 to C7 to predict C_{pr} and θ_{CWC}

Equation	C1	C2	C3	C4	C5	C6	C7	Err
Equation 11 to predict C_{pr}	1.8231	0.1718	0.1214	0.1184	-0.7828	0.9854	-	0.018040
Equation 12 to predict θ_{CWC}	2.4678	-0.1583	0.1066	-0.1897	1.1905	-1.4761	-0.2964	0.004809

Chapter 6

CONCLUSIONS AND RECOMMENDATION FOR FUTURE WORK

6.1 Conclusions

The objective of this study was to find practical and effective way to improve the ductility and strength of post-Northridge connections so that they are better applicable for new and existing buildings. For this purpose multi longitudinal voids were horizontally opened in the beam web where the distance of the centerline of the first pair of voids from the face of the column was equal to the beam depth. All voids had same length (1.25 times the beam overall depth) and same depth. Design parameters α, β and γ were defined to change the geometrical location of the voids. A parametric study was carried out with respect to these parameters to find the optimum location of voids to achieve the highest connection strength and ductility. This finally led to modeling of the 144 post-Northridge specimens of different beam overall depths (SAC7, 5 and 3 with overall depths of 912 mm, 750 mm and 600 mm respectively). Analytical results showed that the presence of the second pair of voids were efficient in uniformly distributing the plastic equivalent strains along the beam length and, therefore, significantly reducing the plastic equivalent strain concentration at the column face level, weld access hole region and at the beam flanges at the void areas. It finally led to the achievement of the adequate strength and ductility for the specimens of the proposed BEC. Results also showed that the

location and size of voids can influence the performance of the modified connections. The effect of the configuration of voids was investigated using design parameters α, β and γ. Results indicated that the highest connection strength and ductility can be achieved for α, β and γ equal to 2, 0.75 and 0.1 respectively. These specimens achieved the minimum required strength. From the ductility point of view, however, the proposed method caused a remarkable increase in the ductility of all connections when compared to the single pair voids (Hedayat and Celikag, 2009). They all achieved the minimum required ductility. On the other hand, the efficiency was better for the deeper beams (overall depth greater than 750 mm) where the deep beam specimens SAC7 (overall depth equal to 912 mm) achieved a remarkable five percent total rotation.

In order to generalize the design procedure to be applicable to any other beam section, the best configuration of voids was estimated, other design parameters were also considered (beam length, beam moment gradient and beam gravity loads) to propose equations 11 and 12. Finally, the best location of voids was controlled by using the parameter η_t. It is expected that any modified specimen (even in the case of a shallow beam) with appropriate value of parameter η_t ($0.95 \leq \eta_t \leq 1.02$) achieves both adequate connection's strength and ductility simultaneously.

6.2 Recommendation for Future Work

In recent years researchers started to look at combination of modifications that has been done so far with regards to improving post-Northridge connections. There is still possibility of further combining the existing methods suggested so far since the research showed that combining methods also further improve the ductility and strength of post-Northridge connections.

In addition, similar methods are advised to be used for different types of moment connections and sections produced according to other standards, such as European sections. There is need to validate more connections around the world so that buildings will be more resistant to earthquakes in countries where there is seismic hazard.

REFERENCES

AISC/ANSI341, Seismic provisions for structural steel buildings, AISC/ANSI341-10, 2010, Chicago (IL), American Institute of Steel Construction, Inc.

ANSI/AISC 360-10 (2010), “Specification for Structural Steel Buildings”, American Institute of Steel Construction.

ANSYS User Manual,. ANSYS, Inc., 2007.

Ascheheim M-A. Moment –resistant structure, sustainer and method of resisting episodic loads. United State Patent, Patent number: 6,012,256; 2000.

Beedle, L. S., Ln, L.-W., and Ozer, E (1973). "Recent developments in steel building design." AISC Engrg. J.; 10(4), 98-111.

Carpenter L. D., and Lu L.-W (1973). "Reversed and repeated load tests of full-scale steel frames." Tech. Rep. Steel Res, for Constr. Bull No. 24, American Iron and Steel Institute, Washington, D.C.

Chan RWK, Albermani F. Experimental study of steel slit damper for passive energy dissipation. Eng Struct 2008;30:1058–66.

Chen CC, Chen SW, Chung MD, Lin MC (2005). Cyclic behaviour of unreinforced and rib-reinforced moment connections. Journal of Constructional Steel Research; 61(1):1–21.

Chen CC, Lee JM, Lin MC. Behavior of steel moment connections with a single flange rib. Engineering structures 2003; 25: 1419-28

Chen CC, Lin CC, Tsai CL. Evaluation of reinforced connections between steel beams and box columns. Engineering Structures 2004; 26, 1889–1904.

Chen, W.-E, and Patel, K. V. "Static behaviour of beam-to-column moment connections." J. Struct. Div., ASCE, 1981, 107(9), 1815-1838.

Chia B, Uang CM, Chen A. Seismic rehabilitation of pre-Northridge steel moment connections: A case Study, (2006). Journal of Constructional Steel Research:62:783–792.

El-Tawil, S., Mikesell, T., Vidarsson, E. and Kunnath, SK. (1998). "Strength and ductility of FR welded-bolted connections", Report No. SAC/BD-98/01, SAC joint venture, Sacramento, CA.

Engelhard, M.D., Uang, C.M., Gross, J.L., Kasai, K. and Iwankiw, N. Modification of existing welded steel moment frame connections for seismic resistance, AISC 2003.

Engelhardt M.D., Uang C.M., Gross J.L., Kasai K., Iwankiw N (2003). Modification of existing welded steel moment frame connections for seismic resistance, AISC.

Engelhardt MD, Sabol TA (1998). Reinforcing of steel moment connections with cover plates: benefits and limitations. Engineering Structures; 20(4–6):510–20.

Engelhardt MD, Sabol TA, Aboutaha RS, Frank KH (1995). Testing connections. Modern Steel Construction, AISC; 35(5):36–44.

Engelhardt MD, Sabol TA. Reinforcing of steel moment connections with cover plates: benefits and limitations. Engineerings structures 1998; 20(4-6) ; 510-520.

Engelhardt MD, Sabol TA. Testing of welded steel moment connections in response of the Northridge earthquake. Northridge steel update 1. American Institute of Steel Construction 1994.

Engelhardt, M. D. and Popov, E. P (1989). 'Behaviour of long links in eccentrically braced frames', Report no. UCB/EERC-89/OI, Earthquake Engineering Research Center, University of California, Berkeley, CA.

Engelhardt, M. D., Winneberger, T., Zekany, A. and Potyraj, T (1996). 'The dogbone connection - Part 11', Modern Steel Construction.

Gates W.E, Morden M (1994). Lessons from inspection, evaluation, repair and construction of welded steel moment frames following the Northridge earthquake. Technical report: Surveys and Assessment of Damage to Building Affected by the Northridge Earthquake of January 17, Rep. No. SAC-95-06, 1995:3-1 to 3-79.

Gilton CS, Uang CM, Cyclic response and design recommendations of weak-axis reduced beam section moment connections, Journal of Structural Engineering, 2002; Vol. 128, No. 4.

Green M. Santa Clarita City Hall (1995): Northridge earthquake damage. Technical Report: Case Studies of Steel Moment Frame Building Performance in Northridge Earthquake of January 17, Rep. No. SAC-95-07, 1995: 1-1 to 1-13.

Hajjar J.F, O'Sullivan D.P, Leon R.T, Gourley B.C (1995). Evaluation of Damage to the Borax Corporate Headquarters Building as a result of the Northridge earthquake. Technical Report: Case Studies of Steel Moment Frame Building Performance in Northridge Earthquake of January 17, 1994. Rep. No. SAC-95-07: 2-1 to 2-76.

Hedayat A.A., Celikag M. Reduced beam web (RBW) connections with circular openings Structural Steel: Shapes and Standards, Properties and Applications**.** New York, USA: Nova Science Publishers Inc; 2010.

Hedayat AA, Celikag M. Post-Northridge connection with modified beam end configuration to enhance strength ductility. Journal of Constructional Steel Research 2009; 65: 1413-30.

Hedayat AA, Celikag M. Wedge design: Reduced Beam Web (RBW) connection for seismic regions. Advances in Structural Engineering 2010; 13(2).

Hedayat AA**,** Saffari H, Eghbali A. Behaviour of steel reduced beam web (RBW) connections with drilled voids. 5th SASTech 2011. Mashhad, Iran: Khavaran Higher-education Institute; 2011.

Hedayat AA**,** Saffari H, Mousavi M. Behavior of steel reduced beam web connections with arch-shape cut. Advances in Structural Engineering. Accepted for publish. In press.

Kasai K, Hodgon I, and Mao C, Bolted repair methods for fractured welded moment connections Proceedings, Behavior of steel structures in seismic areas (Stessa 97) .Kyoto, Japan; 1997, p. 939-946.

Kasai, K., Hodgon, I., and Bleiman, D. (1998). "Rigid-Bolted Repair Methods for Damaged Moment Connections," Engineering Structures, Vol. 20, No. 4-6, pp. 521-532.

Kim T., Whittaker A. S., Gilani A. S. J., Bertero V. V., Takhirov SH. M. Cover-plate & flange-plate reinforced steel moment-resisting connection, repot No. SAC/BD-0027 SAC Joint Venture September 2000.

Mahin SA. Lessons from damage to steel buildings during the Northridge earthquake. Engineering Structures 1998;20(4–6):261–70.

Maleki S. and Tabbakhha M., Numerical study of Slotted-Web–Reduced-Flange moment connection, Journal of Constructional Steel Research, Volume 69, Issue 1, February 2012, Pages 1-7, ISSN 0143-974X.

Manual of steel construction: Load and resistance factor design: volume 1 and 2. 2nd Ed. Chicago: AISC; 1995.

Mao C, Ricles J, Lu L, Fisher J., Effect of local details on ductility of welded moment connections. Journal of Structural engineering 2001;1036-1044.

Miller DK. Lessons learned from the Northridge earthquake. Engineering Structures 1998;20(4–6):249–60.

Naeim F (2001). The seismic design handbook. 2nd ed. Kluwer Academic Publishers; p. 418.

Naeim F, Dijulio R.Jr, Benuska K, Reinhorm A.M, Li C., (1994), Evaluation of seismic performance of an 11-story steel moment frame building during the 1994 Northridge earthquake. Technical report: Analytical and Field Investigation of Building Affected by the Northridge Earthquake of January 17, Rep. No. SAC-95-04, 1995, Part 2: 6-1 to 6-109.

Noel, S. and Uang, C.-M., (1996), "Cyclic Testing of Steel Moment Connections for the San Francisco Civic Center Complex," Report No. TR-96/07, Division of Structural Engineering, University of California, San Diego.

Popov EP, Tsai KC. Performance of large seismic steel moment connections under cyclic loads. Engineering journal, AISC 1998; 26(2): 51-60

Popov EP, Yang T-S, Chang S-P. Design of steel MRF connections before and after 1994 Northridge. Engineering Structures 1998; 20(12): 1030-38.

Popov, E. P., and Bertero, V. V., (1973), "Cyclic loading of steel beams and connections." J. Struct. Div., ASCE; 99(6), 1189-1204.

Popov, E. P., and Pinkney, R. B., (1969), "Cyclic yield reversal in steel building connections." J. Struct. Div., ASCE; 95(3), 327-353.

Popov, E. P., and Stephen, R. M., (1970), "Cyclic loading of full-size steel connections." Tech. Rep. UCB/EERC-70/3, Earthquake Engrg, Res. Ctr., University of California, Berkeley, Calif.

Popov, E. P., and Stephen, R. M., (1972), "Cyclic loading of full-size steel connections." Tech. Rep. Steel Res. for Constr. Bull. No. 21, American Iron and Steel Institute, Washington, D.C.

Recommended seismic design criteria for new steel moment-frame buildings, Report No. FEMA350, 2000.

Recommended seismic design criteria for new steel moment-frame buildings, Report No. FEMA350, 2000.

Ricles J-M, Mao C, Lu L-W, Fisher J-W., Ductile details for welded unreinforced moment connections subject to inelastic cyclic loading. Engineering Structures 2003; 25: 667–680.

Ricles, J.M., Mao, C., Lu, L.W. and Fisher, J.W. (2003),. "Ductile details for welded unreinforced moment connections subject to inelastic cyclic loading", Engineering Structures, Vol. 25, No. 5, pp. 667–680.

SAC (1996) ; Experimental Investigations of Beam-Column Sub assemblages; Technical Report SAC-96-01, Parts 1 and 2, SAC Joint Venture, Sacramento, CA. 739–746

SAC/BD -00/01. Parametric tests on unreinforced connections, volume I-final report. Lee K-H, Stojadinovic

SAC/BD-00/01, Parametric Tests on Unreinforced Connections, Volume I-Final Report, K.-H. Lee, B. Stojadinovic, S. C. Goel, A. G. Margarian, J. Choi, A. Wongkaew, B. P. Reyher, and D.-Y, Lee.

Saffari H, Hedayat AA, Poorsadeghi NejadM. Post-Northridge connections with slit dampers to enhance strength and ductility. Journal of Constructional Steel Research 2013; 80: 138-52.

Specification for structural steel beams with web openings. ASCE standard. SEI/ASCE23-97.

Tsai, K.C. and Popov, E.P., (1993), “Seismic design of steel beam-to-box column connections”, in Proc. Structures Congr. '93, ASCE.

Uang C, Bondad D., (1998), Cyclic performance of haunch repaired steel moment connections: experimental testing and analytical modelling. Engineering Structures (20): 552–561.

Uang CM, Fan CC, (2001), Cyclic stability criteria for steel moment connections with reduced beam section, Journal of Structural Engineering; Vol. 127, No. 9.

Uang C-M, Yu Q-S, Noel S, Gross J., (2000), Cyclic testing of steel moment connections rehabilitated with RBS or welded haunch. J Struct Eng, ASCE; 126(1):57–68.

Uang, C.-M. and Bondad, D. (1996). "Dynamic Testing of pre-Northridge and Haunch Repaired Steel Moment Connections," Report No. SSRP 96/03, University of California, San Diego, La Jolla.

Uang, C.-M., Bondad, D., Noel, S. (1996). Cyclic Testing of the MNH-SMRF™ Dual Strong Axes Moment Connection with Cruciform Column (Report No. TR-96/04), University of California, San Diego, La Jolla, California, U.S.A.

Uang, C.-M., Latham, C. (1995), Cyclic Testing of Full-scale MNH-SMRF™ Moment Connections (Report No. TR-95/01), University of California, San Diego, La Jolla, California, U.S.A.

Wilkinson S, Hurdmanb G, Crowtherb A. A moment resisting connection for earthquake resistant structures. Journal of Constructional Steel Research 2006; 62: 295–302.